UNIVERSITA' DEGLI STUDI DI PARMA
FACOLTA' DI SCIENZE MATEMATICHE, FISICHE E NATURALI
Dipartimento di Biologia Evolutiva e Funzionale
Sezione Fisiologia

TESI DI DOTTORATO DI RICERCA IN
"FISIOPATOLOGIA SISTEMICA"
(XX ciclo)

CARDIAC ELECTROMECHANICAL PERFORMANCE FOLLOWING STEM CELL BASED REGENERATIVE THERAPIES IN INFARCTED RAT HEART

Coordinatore:
Chiar.mo Prof. Ezio Musso

Tutore:
Chiar.mo Prof. Ezio Musso

Dottoranda:
Dott.ssa Monia Savi

ANNI 2005 - 2008

INDEX

INTRODUCTION

Cardiovascular diseases, including myocardial infarction and heart failure, are the leading causes of death in the industrialized world and account for 16.7 million deaths annually. In the United States, approximately 900000 people die every year from the complications of cardiovascular diseases, representing 38% of the overall mortality in this country (www.americanheart.org/statistics). Despite the development of pharmacological and mechanical revascularization techniques, heart failure proceeds as a consequence of myocardial infarction (MI). Left ventricular (LV) remodeling is described as a physiologic and pathologic condition that occurs after acute myocardial infarction (AMI). The process of LV remodeling begins with cardiomyocyte loss due to necrosis or apoptosis and continues with cardiomyocyte lengthening, LV dilation, cardiomyocyte hypertrophy and collagen accumulation [1]. Although cardiac remodeling is initially an adaptive response to maintain normal function, it gradually becomes maladaptive and subsequently leads to progressive decompensation and congestive heart failure (CHF) [2]. The epidemic problem of heart failure, together with the limitations in its management, constitutes the basis for the current interest in regenerative cardiology. This novel field aims at the identification of primitive cells and/or gene products, which are capable of activating directly or indirectly the formation of myocytes and coronary vessels lost because of pathological conditions. The enhancement of the regeneration of cardiomyocytes, as well as stimulation of neovascularization, may prevent cardiac remodeling and the progression of heart failure. Thus, myocardial regeneration appears to be a promising strategy to reduce adverse cardiac remodeling.

Within a few years following the experimental documentation that bone-marrow-derived cells (BMDCs) could induce cardiac repair after infarction, clinicians began to administer endothelial progenitor cells, mononuclear bone marrow cells (BMCs), and CD34-positive cells to patients affected by acute and chronic ischemic heart failure [3-7]. In general, these interventions have had a favorable outcome, pointing to the feasibility and safety of this therapeutic approach. Questions persist, however, concerning the transient and long-term efficacy of this strategy [8-11]. While patients are currently being enrolled in large randomized clinical trials, the documentation for the existence of cardiac-specific progenitor cells (CPCs) has also

raised the possibility of using these resident undifferentiated cells for the treatment of human disease [12, 13].

The notion that the reconstitution of damaged infarcted myocardium cannot be accomplished has been successfully challenged by experimental studies in animals, by using the intramyocardial injection of c-kit^{+} BMDCs, mesenchymal stem cells, embryonic stem cells, endothelial progenitor cells, and systemic mobilization of BMDCs [14]. In all cases, a significant regeneration of the infarcted myocardium has been obtained in combination with an improvement in cardiac function and a decreased mortality [14]. However the most appropriate form of cellular therapy to repair myocardial injury remains to be identified.

Recent data have shown that the adult heart from rat, dog, pig and, most importantly from humans, possesses a subpopulation of undifferentiated cells expressing the surface antigens c-kit, MDR-1 and SCA-1 [15-19], typically present in hematopoietic stem cells [20-23]. The finding that these cells (resident cardiac stem cells: CSCs) are able to differentiate into the three major cardiac cell types including myocytes, smooth muscle cells and endothelial cells [18, 24, 25] has dramatically challenged the generally accepted but never proven paradigm that the heart is a post-mitotic organ. Clinically, it might be more efficient and powerful to employ stem cells that reside in the damaged organ than to deliver cells from the bone marrow and other sources. By necessity, non cardiac progenitor cells have to undergo a reprogramming phase to acquire the cardiomyocyte lineage and to generate coronary vessels [26]. The natural pathways of differentiation and stability of the original phenotype are preserved when stem cells are located in their developmentally determined microenvironment [27]. CSCs are predestined to become myocardial cells, and this inherent advantage overcomes the need for complex and time-consuming process of chromatin reorganization. This may suggest that CSCs are more efficient than other stem cells in promoting cardiac regeneration. In addition, CSCs will exhibit a prompt growth response to the treatment and therefore a quick recovery of cardiac mass and function. Recent studies performed in rat [24] and mouse models [28] have shown that when CSCs are injected directly into the myocardium adjacent to the infarct, produced by a permanent coronary occlusion, they migrate to the infarct and reconstitute part of the dead tissue, reducing infarct size and ameliorating cardiac function. Similar results have

been obtained by intravascular delivering of CSCs, in rat models with temporary coronary occlusion followed by reperfusion [29].

The possibility of promoting cardiac tissue regeneration through growth-factor-mediated CSC activation has been recently addressed. CSCs express receptors for a variety of growth factors (GFs), cytokines, and chemokines; these include: (i) c-Met, the receptor for Hepatocyte Growth Factor (HGF); (ii) the receptor for Insulin-like Growth Factor-1 (IGF-1); (iii) flk-1, the receptor 2 for Vascular Endothelial Growth Factor (VEGF), (iv) CXCR4, the receptor for Stromal Derived Factor-1 (SDF-1) [30]; and (v) the receptor for advanced glycation end products (RAGE) which is also activated by the cytokine high mobility group box 1 (HMGB1) [31]. Therefore, growth factor treatment may modulate CSC function.

Recently, IGF-1 and HGF have been used in combination in order to stimulate the migration of resident CSCs to the infarcted area of the heart and to promote their proliferation and survival. These experiments were performed in mice [32] and dogs [30], in which CSCs were isolated and characterized. IGF-1 plays an important role in the homeostasis of the CSC compartment. IGF-1 is mitogenic, anti-apoptotic, and necessary for neural stem cell growth [33]. IGF-1 promotes myocyte formation and attenuates myocyte death after infarction [34]. Selective over-expression of the IGF-1 transgene in the heart promotes cardiomyocyte formation and reduces myocyte death after infarction [35,36]. In the aging myocardium, the IGF-1/IGF-1R system increases CSC proliferation and reduces CSC apoptosis. These two processes lead to a delay in the senescence of CSCs, increasing their number and functional competence.

HGF may promote cell migration [37] in various organs, including the brain and to a lesser extent, cell growth and survival. Cell locomotion is activated by the expression and the activation of matrix metalloproteinases (MMPs) [38] that by breaking down the extra-cellular matrix favor cell locomotion, homing and tissue reconstitution. In vitro studies show that HGF is a powerful CSC chemo-attractant, more effective than Fibroblast Growth Factor-2 (FGF-2), granulocyte-macrophage colony stimulating factor (GM-CSF), Epidermal Growth Factor (EGF), VEGF and Stem Cell Factor (SCF). On the other hand, IGF-1 shows little effect on CSC migration but has a predominant role in promoting their proliferation and survival. The administration of HGF and IGF-1 in murine and canine infarcted hearts, induced CSC migration in the

injured region where they differentiated into cardiomyocytes and coronary vessels. Myocardial regeneration was characterized by the formation of immature cardiac cells that possess a fetal-neonatal phenotype. However, in both animal models, in response to the treatment with HGF and IGF-1, there was echocardiographic evidence of contraction in the infarcted region, and hemodynamic studies documented an improvement in cardiac mechanical function [32, 30]. These results were confirmed by another study performed in rats, in which the regenerative response of resident CSCs was documented after the local injection of HGF and IGF-1 in chronic infarcts [39].

Most data indicate that the mechanical performance of the damaged heart is improved by stem cell therapy [40]. However a wide use of cardiac regenerative therapies in the clinical setting requires a knowledge of the electrophysiological consequences of the regenerative therapies. This implies that research topics should include a thorough analysis of both the contractile function and the electrogenesis of the repaired heart. The building of appropriate electrical connections between the regenerated myocardium and the spared surrounding tissue is crucial for the achievement of a complete recovery of normal cardiac function. The fulfillment of these conditions constitutes a fundamental step in the evaluation of therapeutic efficiency of stem cell treatment in cardiac research. By contrast, only fragmented information is available so far and no comprehensive study exists aimed at establishing whether the improvement of cardiac mechanical function induced by stem cell treatment is associated with increased, reduced or unchanged arrhythmia vulnerability.

Proarrhythmia after stem cell therapy might be attributed to several reasons and the precipitating mechanisms have been recently analyzed [41]. They include: 1) heterogeneity of action potentials between cells from spared myocardium and transplanted/mobilized stem cells; 2) intrinsic arrhythmic potential of injected/mobilized stem cells; 3) increased and heterogeneous autonomic nerve sprouting induced by stem cell based treatment; and 4) local injury or edema induced by intramyocardial stem cell injection/mobilization. The nature of the injected cell may have the most impact on arrhythmogenesis after transplantation. For instance, myoblasts (precursors of skeletal muscle cells) and bone marrow derived stem cells differ in their inherent electrophysiologic properties and ability to couple electromechanically among themselves and with host cardiomyocytes. The limited clinical data so far available

suggest that arrhythmias are more likely to occur after myoblast transplantation [42-44] while proarrhythmic effects of bone marrow derived stem cell injection may be transient [41, 45-49]. Thus, more effort has to be made to establish whether amelioration of mechanical performance of hearts submitted to regenerative therapies is associated with reduction of proneness to arrhythmias. Because the occurrence of cardiac arrhythmias is highly unpredictable, experiments must be designed which allow an accurate evaluation of the electrical competence of the repaired heart at the organism, tissue and cellular/ molecular levels, in order to understand the natural course of the risk of arrhythmias during stem cell treatment.

This issue was specifically addressed in the present study, in a rat model of chronic myocardial infarction. The importance of studying chronic MI resides in the fact that: (i) ventricular remodelling following MI represents a major cause of late infarct-related heart failure, and (ii) lethal arrhythmias are responsible for up to half the deaths in heart failure. Two different experimental approaches were used in order to regenerate the dead tissue by stem cell based treatment: 1) in situ activation of resident progenitors by local injection of growth factors (HGF and IGF-1); 2) local injection of cardiac stem cells with or without the addition of HGF and IGF-1.

MATERIALS and METHODS

Animals and housing

The study population consisted of male Wistar rats (*Rattus norvegicus*) breed in our departmental animal facility, age 12-14 wk, weighing 350 - 400 g. Animals were kept in unisexual groups of four individuals from weaning (4wk after birth) until the onset of the experiments, in a temperature-controlled room at 22–24 °C, with the light on between 7.00 AM and 7.00 PM. The bedding of the cages consisted of wood shavings, and food and water were freely available. The investigation was approved by the Veterinary Animal Care and Use Committee of the University of Parma and conformed with the National Ethical Guidelines (Italian Ministry of Health; D.L.vo 116, January 27, 1992) and the Guide for the Care and Use of Laboratory Animals (NIH publication no. 85–23, revised 1996).

General outlines of the experimental protocol 1 (EP-1)

The details of the various procedures employed will be provided below in separated paragraphs.

Seventy rats were divided in 3 groups. (1) MI-GF (n=27), animals subjected to myocardial infarction (MI) and treated four weeks later with growth factors (GFs); (2) MI-V (n=28), animals with myocardial infarction treated with growth factor vehicle (V); (3) SO-V, animals (n=15) subjected to sham operation (SO) and treated with growth factor vehicle. The growth factors were Hepatocyte Growth Factor (HGF) and Insulin-Like Growth Factor-1 (IGF-1).

- In MI-GF (n=22), MI-V (n=23), and SO-V (n=15) animals, vulnerability to arrhythmias and cardiac mechanical performance were evaluated one month after surgery (induction of infarction or sham operation) by means of (i) telemetry ECG recording during stress-induced autonomic stimulation (social stress procedure) [50] and (ii) echocardiography. The same measurements were repeated 15 days after intra-myocardial injections of GFs or vehicle. Finally, hemodynamic data were invasively collected and the heart of each animal was perfusion fixed for morphometrical and immunohistochemical studies.
- The hearts of the remaining 10 rats (MI-GF, n=5; MI-V, n=5) was frozen and used for electrophoretic and immunoblot assay.

General outlines of the experimental protocol 2 (EP-2)

The details of the various procedures employed will be provided below in separated paragraphs.

Myocardial infarction was produced in 56 animals, under anesthesia. Seven rats died after ligature and three after anesthesia leaving a total of 46 animals. One month later, 17 rats (MI-cells group), were treated with implantation of clonogenic cardiac progenitor cells isolated from Enhanced-Green Fluorescent Protein (EGFP)-rats (EGFP-CPCs), 19 animals (MI cells+GF group) with EGFP-CPCs supplemented with HGF and IGF-1, and the remaining 10 rats with saline (MI-saline group). Simultaneously with growth factor (GF) or vehicle administration, selected subgroups of MI-cells, MI-cells+GF and MI-V rats were also treated with BrdC, to detect regenerative processes. Two weeks later, hemodynamic measurements were collected and, at sacrifice, hearts were perfusion-fixed for cardiac anatomy, morphometry and immunohistochemical analysis. To study the electrophysiological consequences of cell transplantation, 32 rats belonging to the original 46, were also chronically instrumented with a miniaturized transmitter for telemetry ECG recording. After one week, a 30-min continuous baseline ECG was recorded to verify the spontaneous proneness to arrhythmias. Then myocardial infarction was induced and three weeks later the animals were investigated for vulnerability to arrhythmias occurring during stress-induced autonomic stimulation (social stress: resident-intruder test) [50]. Afterwards, all animals were injected with: (i) EGFP-CPCs alone (MI-cells group; n=10), (ii) EGFP-CPCs added with GFs (MI cells+GF group; n=12) and (iii) saline (MI-saline group; n=10). Thirteen days later, telemetry ECG recording was repeated to determine the effects of treatment on the arrhythmogenesis.

Fifteen additional animals were submitted to sham operation (SO) and treated with EGFP-CPCs alone (SO-cells; n=8) or with EGFP-CPCs supplemented with GFs (SO-cells+GF; n=7). The two groups of animals underwent the same experimental protocol to test the electrophysiological consequences of stem cell based treatments in normal heart.

Chronic instrumentation for telemetry ECG recording (EP-1 andEP-2)

Animals were chronically instrumented with a miniaturized transmitter for telemetry ECG recording (model TA11CTA-F40, Data Sciences, St Paul, MN). The details of the surgical procedure have been published [51].

Briefly, each rat was anaesthetized with ketamine chloride (Imalgene, Merial, Milan, Italy; 40mg/kg ip), plus medetomidine hydrochloride (Domitor, Pfizer Italia S.r.l., Latina, Italy; 0.15 mg/kg ip). A ventral celiotomy was performed and the body of the transmitter was placed into the abdominal cavity. One recording lead was fixed to the dorsal aspect of the xiphoid process, close to the apex of the heart. The other lead was subcutaneously tunnelled on the thorax toward the upper insertion of the sternohyoid muscle. Here, the wire was formed into a U shape, pushed under the muscle and then along the trachea into the anterior mediastinum, to get the tip of the recording lead close to the right atrium. Finally, the muscle and skin layers were separately sutured.

After surgery, all animals were given atipamezole hydrochloride (Antisedan, Pfizer Italia S.r.l., Latina, Italy; 0.15 mg/kg im), flunixin (Finadyne, Schering-Plough S.p.a, Milan, Italy; 5 mg/kg im), gentamicine sulphate (Aagent, Fatro, Milan, Italy; 10mg/kg im) and kept warm with infrared lamp radiation. All animals were given antibiotic therapy for the 3 subsequent days and individually housed.

Social stress procedure and telemetry ECG data acquisition and processing (EP-1 and EP-2)

Social stress was obtained by the resident–intruder test paradigm [50] which consists of introducing the instrumented animal (intruder) into the territory of an unfamiliar conspecific male (resident) belonging to an aggressive wild strain of rats (Rattus norvegicus, Wild Type Groningen, WTG). This procedure is known to produce an intense activation of the sympathetic–adrenomedullary system and the hypothalamic–pituitary–adrenocortical axes [52]. High levels of aggression by the resident animal were achieved and maintained by cohabitation with a female and a training procedure accomplished in the 2 weeks preceding the intruder test.

All experimental session were performed during the light phase, between 9.00 AM and 1 PM. Each session consisted of two successive 15 min continuous ECG recordings which were performed while the instrumented animal was respectively: (i) left alone and undisturbed in its home cage (baseline conditions) and (ii) exposed to the social stress procedure (test period). The ECG signals were collected by a receiver (model CTR85-SA, Data Sciences) placed under the experimental cage, monitored on an oscilloscope and simultaneously routed to a personal computer via an analog-to-digital conversion board (1 kHz sampling rate) for permanent storage.

The ECG data were then processed by using a custom made software package for interactively analyzing heart rate behavior and detecting ventricular arrhythmic events (VAEs).

Myocardial infarction and sham operation (EP-1 and EP-2)

Rats, anesthetized with Imalgene+Domitor as previously described, were intubated with a properly modified 16-gauge needle, artificially ventilated (Rodent ventilator UB 7025, Ugo Basile, Comerio, Italy), and treated with gentamicine sulphate (Aagent, Fatro, Milan, Italy; 10mg/kg im). Then, with the aid of a dissecting microscope, a thoracotomy via the third-left intercostal space was performed and a 5-0 silk suture was passed with a tapered needle under the left anterior descending coronary artery, 2-3 mm from the tip of the left auricle and tied securely. After ligation, successful infarction was immediately evident by a pale discoloration of left ventricular myocardium due to ischemia. The chest was then closed in layers, and a small catheter was introduced in the thorax to evacuate air and fluids.

The rats were given Antisedan, removed from the ventilator, kept warm with infrared lamp radiation and eventually individually housed. Antibiotic therapy was given during the subsequent 3 days. Sham-operated rats were treated similarly, except that the ligature around the coronary artery was not tied.

HGF and IGF-1 administration and BrdC delivery (EP-1)

Four weeks after coronary ligature, left lateral thoracotomy was repeated in all animals under anesthesia and mechanical ventilation as described above. In MI-GF rats six injections with increasing concentrations of HGF (PeproTech EC, London, UK) and constant concentration of IGF-1 (PeproTech EC) were done. The first injection was located near the atria, the second between the atria and the infarct and the last four at opposite sites of the border zone. Sham-operated and infarcted-untreated rats were injected with saline.

The sterile solution of growth factors contained different concentration of HGF (atria: 50ng/ml; atria-border zone: 100ng/ml; opposite sites of border zone: 200ng/ml) and constant concentration of IGF-1 (200ng/ml in all six injection sites) diluted in saline (phosphate buffer solution: PBS). In MI-GF rats, Rhodamine microspheres, 2.0 μm in diameter (FluoSpheres, Molecular Probes, Eugene, USA), were added to the solution (microsphere solution volume: 5% of the total volume injected) to ensure the successful injection. Each injection consisted of 10 μl. A scheme illustrating this protocol has been published [32].

In order to quantify the regenerative processes by immunohistochemical analysis, selected subgroups of MI-GF (n=14) and MI-V (n=11) rats were simultaneously implanted with an osmotic pump (model 2ML4, ALZET, Charles River, Italy) placed subcutaneously in the interscapular region for continuous infusion of 0.6M BrdC (MP Biomedicals Europe, Asse-Relegem, Belgium) with a delivery rate of 2.5 μl/h. Infusion was maintained until the animals were killed (15 days). The long infusion time prompted us to use BrdC rather than BrdU, usually employed for the detection of newly formed cells, because of the nearly six fold higher solubility of BrdC (which is metabolically converted to BrdU, in vivo).

Cell isolation and culture (EP-2)

CPCs were isolated from the hart of enhanced-Green Fluorescent Protein (EGFP)-rats kindly provided by Dr Okabe [53] at 3 month of age. Cell isolation was processed as described in Beltrami et al. *Cell* 2003 [24] with minor modifications.

CPCs were isolated from the whole heart by Langhendorff perfusion apparatus as previously described [54]. Briefly, the rat heart still beating was quickly excised from anesthetized (Imalgene+Domitor) and heparinized (100 UI/kg) animals and hanged by an aortic cannula to the perfusion system. The heart vasculature was first washed out by a perfusion buffer and then perfused with Collagenase type II solution at 37°C. At the end of collagenase, the heart was minced and put in a shaking albumine solution at 37°C to allow mechanical tissue digestion. The solution containing all cells was washed several times, centrifuged at 300 rpm to remove cardiomyocytes and then submitted to Percoll (Sigma, Italy) gradient to further enrich the fraction of small cells. The cell layer visualized at the interface of the desired gradient was centrifuged at 1000 rpm and cells re-suspended in 10 ml of culture medium containing Iscove Modified Dulbecco's Medium (IMDM, Sigma, Italy) supplemented with 1% Penicillin-Streptomycin (P/S, Sigma, Italy), 1% Insulin-Transferrin-Sodium Selenite (I/T/S, Sigma, Italy), 10% Fetal Bovine Serum (FBS, Sigma, Italy) and 10 ng/ml Basic-Fibroblast Growth Factor (b-FGF, Sigma, Italy) and seeded in Petri dishes (Corning, USA) placed at 37°C-5% CO2 for their amplification.

Daily, microscopic observation of cultures showed the growth of two different adherent cell populations, one with mesenchymal-like and one with monomorphic blast-like characteristics. This latter population constituted so-called Cardiac Progenitor Cells (CPCs) provided by clonogenic growth and multipotency. These cells were amplified for several passages and cryo-preserved in aliquots in a medium composed by FBS supplemented with 1% Dimethylsulphoxide (DMSO, Sigma, Italy) when needed for our experimental plan.

Cell Tracking (EP-2)

To detect homing and engraftment of the injected cells into murine hearts, EGFP-CPCs were processed using the following protocol before their injection.

Quantum Dots (QDots)

QDot nanocrystals are fluorophores-substances that absorb photons of light, then re-emit photons at a different wavelength. However, they exhibit some important

differences as compared with traditional fluorophores, such as organic fluorescent dyes and naturally fluorescent proteins. QDot nanocrystals are nanometer-scale (roughly protein-sized) atom clusters, containing from a few hundred to a few thousand atoms of a semiconductor material (cadmium mixed with selenium or tellurium), which has been coated with an additional semiconductor shell (zinc sulphide) to improve the optical properties of the material. These particles fluoresce in a complete different way in comparison with traditional fluorophores, without the involvement of π-> π * electronic transitions.

Different nanocrystal solutions could be excited by the same UV wavelength lamp showing different colour emissions. The difference depends on the size of the nanocrystal.

We employed Qtracker® 585 Cell Labeling Kit (QDots, Invitrogen, Italia), possessing an emission at 585 nm wavelength able to show QDots in yellow fluorescence after UV lamp excitation.

CPCs were stained with Qtracker® 585 Cell Labeling Kit which uses a custom targeting peptide to deliver yellow-fluorescent QDot® 585 nanocrystals into the cytoplasm of living cells. Once inside cells, Qtracker® labels provide intense, stable fluorescence that can be traced through several generations, and they are not transferred to adjacent cells in a population of growing cells, enabling long-term studies of live cells and tissues. The protocol was performed following manufacture's suggestions.

In order to evaluate the fate and distribution of QDots in growing cells in vitro, CPCs at P4 were seeded at concentration of 6000/cm^2, stained with QDots and plated in chamber slides. The cells were then fixed, as previously described, after 24 hours, one week and 3 weeks after plating. The area occupied by QDots in each cell and the fraction of labeled cells was determined using a software for image analysis (Image Pro-Plus 4.0, Media Cybernetics, USA) connected to the fluorescence microscope.

CPCs injection and BrdC delivery (EP-2)

Four weeks after coronary ligature, left lateral thoracotomy was repeated in all animals under anaesthesia (Imalgene+Domitor) and mechanical ventilation as described above. A group of rats was treated with EGFP-CPCs. Specifically, 6X10^5 QDots stained

EGFP-CPCs suspended in 300 μl of IMDM+1% PS were delivered in three regions bordering the scar. In another group of rats, QDots stained EGFP-CPCs were supplemented with HGF (200ng/ml) plus IGF-1 (200ng/ml) and administered in the same way. Each injection consisted of 100 μl. Infarcted untreated animals received equal volumes of saline.

Simultaneously to the injections, subgroups of animals were implanted with a subcutaneous osmotic pump for BrdC delivery, as described above, for the quantitative assessment of cumulative cell proliferation by immunohistochemistry.

Echocardiographic measurements (EP-1)

Serial echocardiograms were obtained in rats under anesthesia (Imalgene+Domitor), using a Vivid 7 echocardiography machine (GE Medical Systems, Madison, WI, USA) equipped with 10 - 7 MHz phased array transducers. The anterior chest was shaved and the animals were placed in prone position. Two-dimensional (2-D) and M-mode images were recorded from modified parasternal long axis and parasternal short-axis views.

Diastolic and systolic anatomical parameters were obtained from M-mode tracings at the mid-papillary level. The measurements included: (i) end-diastolic and end-systolic left ventricular diameter (LVEDD and LVESD, respectively); (ii) end-diastolic and end-systolic thickness of the inter-ventricular septum (IVSD and IVSS); (iii) thickness of the left ventricular posterior wall (LVPW); (iv) end-diastolic and end-systolic left ventricular volume (LVEDV and LVESV) and (v) ejection fraction and fractional shortening (EF, FS).

Hemodynamic studies (EP-1 and EP-2)

Rats were anesthetized with droperidol + fentanyl citrate (Leptofen, Farmitalia-Carlo Erba, Milan, Italy; 1.5mg/kg im) which we have found to induce negligible changes in cardiovascular parameters, telemetrically recorded in conscious animals (unpublished data). Then, a microtip pressure transducer (Millar SPC-320, Millar, Houston, TX, USA) connected to a recording system (Power Laboratory ML 845/4

channels, 2Biological Instruments, Besozzo-Varese, Italy) was inserted into the right carotid artery to record systolic and diastolic blood pressure. The pressure transducer was then advanced into the left ventricle to measure: (i) left ventricular systolic (LVSP) and end-diastolic pressure (LVEDP) and (ii) maximum rate of ventricular pressure rise (+dP/dt) and reduction (-dP/dt), taken as indices of LV contractile performance (software package CHART B4.2).

Anatomical parameters (EP-1 and EP-2)

The hearts of anesthetized animals were arrested in diastole by injection of 5 ml cadmium chloride solution (100 mmol, iv) and the myocardial vasculature shortly perfused at a physiological pressure with a heparinized PBS-solution, followed by perfusion with 10% formalin solution. The heart was then excised and placed in formalin solution (10%) for 24 hours.

Then, the right ventricle (RV) and the left ventricle (LV) inclusive of the septum were separately weighed and the volume of the left ventricular myocardium was computed by dividing LV weight by the specific gravity of the tissue (1.06 g/ml). The major cavitary axis of the LV was measured from the aortic valve to the apex, under a stereomicroscope with a ruler calibrated exactly to 0.1μm (Biological Instruments, Italy). Subsequently, the heart was sliced in three 1-mm thick transversal sections, at the basal, equatorial and apical levels of the ventricle. On the equatorial section, LV wall thickness and LV chamber diameter were morphometrically determined using a software for image analysis (Image Pro-plus 4.0). LV chamber volume was calculated according to the Dodge equation which equalizes the ventricular cavity to an ellipsoid [55]. Afterwards, the sections were embedded in paraffin. Five-μm thick slices were finally cut from the equatorial portion of the LV free wall for morphometric and immunohistochemical studies.

Morphometric analysis

a) Infarct Size (EP-1 and EP-2)**.** The infarcted portion of the ventricle was easily identifiable grossly and histologically. In MI animals, the area of the damaged tissue

from the endocardial to the epicardial layer and the total area of the viable myocardium were measured in the three slices corresponding to the base, mid-region and apex indicated above. Due to shrinkage of the infarcted region and ongoing myocyte growth and death within the viable myocardium, the computation of the number of lost and remaining myocytes after infarction provides a more appropriate characterization of infarct size and extent of recovery with time. The number of myocytes in the LV of control and infarcted hearts was obtained employing a methodology well-established in our laboratory [56, 57].

The quotient between the number of myocytes present in the infarcted LVs and the number of LV myocytes in sham-operated animals gives the percentage of myocytes lost after infarction. The percentage of myocytes lost provides a quantitative measurement of infarct size while the percentage of myocytes left correlates with ventricular function. The newly-formed myocardium in treated-hearts was not included in this analysis in order to evaluate the consequences of coronary ligation on infarct size, independently from tissue reconstitution.

b) Collagen accumulation in the spared LV (EP-1). Five-micrometer-thick sections from the equatorial slice of the LV (see above) were stained with Masson's trichrome and analyzed by optical microscopy (magnification 250X) in order to evaluate in the remote spared myocardium: (i) the volume fraction of myocytes, (ii) the volume fraction of fibrosis, and (iii) the numerical density and average cross-sectional area of fibrotic foci.

According to a procedure previously described [58], for each section, a quantitative evaluation of the volume fraction of myocytes and fibrotic tissue was performed in 60 adjacent fields from sub-endocardium, mid-myocardium and sub-epicardium. The measurement was obtained with the aid of a grid defining a tissue area of 0.160 mm^2 and containing 42 sampling points each covering an area of 0.0038 mm^2. To define the volume fraction of fibrosis, the number of points overlying myocardial fibrosis was counted and expressed as percentage of the total number of points explored.

c) Myocyte Cell Size (EP-1). In sections of 10 MI-V and 12 MI-GF hearts, the cross sectional area of myocytes was morphometrically determined by measuring the

cell diameter, at the nucleus level, in transversally oriented myocytes. For each heart, 120 to 250 cellular measurements were performed.

Immunohistochemical analysis (EP-1)

Five-micrometer-thick sections (see above) obtained from 10 MI-GF+BrdC and 10 MI-V+BrdC rat hearts with comparable infarct size were analyzed to determine: (i) the expression and spatial distribution of Connexin-43 (Cx43) and N-cadherin, and (ii) the incidence of c-kit^{pos} CSCs and the fraction of nuclei labeled by BrdU, in the infarcted, peri-infarcted and remote LV myocardium.

BrdU, c-kit, Cx43 and N-cadherin labeling was detected by immunofluorescence. LV sections were incubated with the primary antibody (monoclonal mouse anti-BrdU antibody, dilution 1:20, Dako, Glostrup, Denmark; rabbit polyclonal anti-c-kit antibody, dilution 1:20, Santacruz; mouse monoclonal anti-Cx43 antibody, dilution 1:250, Chemicon, Temecula, CA, USA; rabbit polyclonal anti-N-cadherin antibody dilution 1:200, Calbiochem, San Diego, CA, USA)**.** Myocytes and smooth muscle cells were identified by staining the same sections respectively with monoclonal mouse anti-α-sarcomeric actin antibody (anti-α-SARC; dilution 1:30, Dako) and monoclonal mouse anti-α-smooth muscle actin antibody (anti-α-SMA; dilution 1:50, Dako). FITC, TRITC-, Cy5- conjugated anti-mouse or anti-rabbit secondary antibodies (Jackson Laboratory, Baltimore, PA, USA) were used to detect simultaneously the different epitopes. Nuclei were recognized by bisbenzimide staining (Hoechst n. 33258, Sigma, St Louis, MO, USA).

Quantitative measurement of newly formed myocardium. The amount of newly formed myocardium was computed by calculating the number and size of small α-SARC positive myocytes according to a methodology previously employed in our laboratory [59].

Moreover, the number of resistance arterioles was measured by counting vascular profiles labeled by α-SMA within the infarcted myocardium.

Immunohistochemical analysis (EP-2)

The number of engrafted CPCs and CPC differentiation were determined by immunohistochemistry.

Enhanced Green Fluorescence Protein (EGFP), BrdC, alpha-sarcomeric actin (α-SARC), alpha-smooth muscle actin (α-SMA) and Connexin 43 (Cx43) were detected by specific antibodies and immunofluorescence. For this purpose, LV sections were incubated with the primary antibody (polyclonal goat anti-GFP, dilution 1:100, Abcam, UK; monoclonal mouse anti-α-SARC, dilution 1:100, Sigma, Italy; monoclonal mouse anti-α-SMA, dilution 1:100, Neomarkers, Italy; mouse monoclonal anti-Cx43, dilution 1:250, Chemicon, USA). FITC-TRITC conjugated specific secondary antibodies were used to simultaneously detect different epitopes. Nuclei were recognized by the blue fluorescence of DAPI (4',6-diamidine-2-phenyndole, Sigma, Italy) staining.

Moreover, the number of arterioles was measured by counting vascular profiles labeled by α-SMA in the infarcted area.

Electrophoretic and immunoblot analysis (EP-1)

The infarcted and non-infarcted portion of the LV ventricles obtained from 5 MI-GF and 5 MI-V animals were weighted and immediately frozen at -80 C°. For immunoblot assay of Cx43, the fresh ventricular tissue was lysed with 150-200 μl of lysis buffer containing the following (SIGMA, St Louis, MO, USA): protease inhibitor dithiothreitol (0.5mM), DNase (50μg/ml), RNase (50μg/ml), HEPES (10mM), NaCl (400mM), EGTA (0.1mM), glycerol (5%), NP40 (3%). Equivalents of 100-125 μg of protein were separated by 10.5% SDS-PAGE, transferred on nitrocellulose filters and exposed to anti-Cx43 monoclonal mouse antibody (dilution 1:750, Chemicon). Binding sites were detected by peroxidase-conjugated specific anti-mouse IgG (dilution 1:2000, in ECL reagents; Amersham Biosciences**,** Piscataway, NJ, USA). The intensity of the bands representing the connexin protein was quantified using a densitometer (Molecular Dynamics, Sunnyvale, CA, USA) and the data were expressed as optical density units.

Statistical analysis

The SPSS statistical package was used (SPSS, Chicago, IL, USA). Normal distribution of variables was checked by means of the Kolmogorov-Smirnov test. Statistics of variables included mean ± standard error (S.E.M.), paired Student t-test, one- way analysis of variance (post-hoc analyses: Bonferroni test or Games-Howell test, when appropriate), and linear correlation analysis. Statistical significance was set at $p<0.05$.

RESULTS of EXPERIMENTAL PROTOCOL 1

IN VIVO STUDIES

Telemetry ECG recordings

R-R interval and indirect measurements of the autonomic input to the heart. The average values of most parameters relating to heart rate did not show any significant differences among groups, before and after GFs/V-injection suggesting that growth factor administration did not markedly affect heart rate and autonomic modulation of the regenerated heart (Table 1). In all groups, the stress procedure increased heart rate (1/R-R interval) by 26-32 % and reduced SD_{RR} and r-MSSD by 37-48% and 27-39% respectively ($p<0.01$; Table 1), as a result of the enhanced sympathetic activity induced by social stress [52, 60].

Proneness to arrhythmias. In all animals, ventricular arrhythmias mostly consisted of isolated premature beats and a few couplets although in some instances more complex patterns could be found (Figure 1). Therefore, arrhythmia vulnerability was evaluated as number of ventricular arrhythmic events (VAEs) during the 15-min baseline and stress periods. Before GFs/V injection, baseline VAEs were negligible in all groups and were significantly increased by social stress. However, the increment of stress-induced VAEs was about two-fold higher in MI as compared with SO rats ($p<0.05$; Figure 2). Fifteen days after GFs/V injection, baseline VAEs remained unchanged in all groups while stress VAEs were markedly reduced in MI-GF rats (-55.8%; $p<0.05$) but not in SO-V and MI-V animals (Figure 3B). Thus, cytokine treatment lowered the proneness to arrhythmias triggered by sympathetic stimulation in conscious infarcted animals.

Echocardiographic measurements

Before GFs/V-injection, in all infarcted rats echocardiographic parameters indicated a global deterioration of cardiac anatomy and function as compared with SO group ($p<0.05$; Table 2). In addition to a reduced ejection fraction and fractional shortening (-8.6% and -14.6% respectively), a marked increase in chamber volume was observed in MI group (LVEDD: +16%; LVEDV: +57%; Table 2).

In MI-V animals, fifteen days after vehicle injection, the morpho-functional properties of the left ventricle either remained unchanged or underwent a slight further deterioration (Figure 4). In contrast, in MI-GF rats cytokine injection was followed by an improvement of echocardiographic parameters whose average values approached in some cases (LVEDD and LVEDV) those measured in SO-V group (Figure 4) suggesting a positive effect of GFs treatment on left ventricular remodeling. As expected, in MI-V group the magnitude of myocardial damage dictated the deterioration of ventricular structure and contractile function.

This was indicated by the finding that the extension of the infarcted area was negatively correlated with fractional shortening and ejection fraction (Figure 5A, B) and positively correlated with left ventricular end-systolic diameter and end-systolic volume (Figure 5C, D). In contrast, these correlations disappeared in MI-GF group further supporting the hypothesis that the administration of GFs induced a partial recovery of ventricular mechanical performance (Figure 6A÷D). Indeed, GFs-mediated regenerative processes, by adding more mechanically efficient myocardial mass might render ventricular contractility independent of infarct size.

Hemodynamic studies

Hemodynamic measurements were characterized by a substantial reduction in systolic ventricular pressure and the peak positive and negative ventricular dP/dt in MI-V and MI-GF groups as compared with SO-V (Table 3).

Interestingly, in accordance with echocardiographic data, the deterioration of ventricular contractility and the degree of LV chamber dilation (as measured by +dP/dt and LVEDP) were correlated with infarct size only in MI-V group (Figure 7A, B). Conversely, the two relationships were lost in MI-GF group (Figure 7C, D) confirming that GF treatment renders the alterations of LV structure and mechanical performance independent of the magnitude of damaged myocardium.

POST MORTEM STUDIES

Cardiac Structure

We tested whether the beneficial effects of cytokine treatment on the electro-mechanical properties of the infarcted heart had a structural-anatomical counterpart.

Gross Cardiac Anatomy. Compared with SO-V animals, MI-V group exhibited a significant increase in chamber volume associated with thinning of the left ventricular wall, resulting in a decreased mass-to-chamber volume ratio (Table 4). Chamber dilation and unfavorable LV remodeling, representing the major anatomical determinants of heart failure, were markedly attenuated in MI-GF rats (Table 4).

Morphometric Measurements

Myocardial fibrosis and small foci of collagen accumulation uniformly distributed throughout the LV wall were measured in the remote non-infarcted left ventricular myocardium of MI-V and MI-GF groups. However, the volume fraction of interstitial fibrosis and the number of foci of replacement fibrosis was more than 2-fold lower in treated MI-GF hearts ($p<0.01$; Figure 8).

Myocyte Cell Size. Measurement in tissue sections of cross sectional area of spared myocytes showed that average cell size was increased by myocardial infarction as compared with SO, however a statistically significant difference was reached only in MI-V (SO-V: 311.1 $\mu m^2 \pm 10$; MI-V: 436±18; MI-GF: 362±19; $p<0.05$ SO vs. MI-V), indicating that reactive cellular hypertrophy was attenuated by intramyocardial injection of GFs.

Immunohistochemical analysis of myocardial regeneration

Myocardial regeneration was characterized by areas of newly formed myocardium present in the infarcted and peri-infarcted portion of treated rat hearts. As shown in Figure 9A-B, small BrdU positive myocytes expressing N-Cadherin and Cx43 were observed indicating that intramyocardial injection of GFs was able to activate the

differentiating properties of resident progenitor cells. More than 3-fold increase in cycling myocytes, in the infarcted myocardium, was observed in MI-GF compared with MI-V (Figure 10).

Importantly, the newly formed tissue was properly perfused as indicated by a 2-fold increase in BrdU positive smooth muscle cells constituting arteriolar profiles (Figure 11A, B). A similar increase was also observed for endothelial cells (data not shown). Formation of electro-mechanically competent myocytes and vascular structures was also present in the remote myocardium (Figure 12) of treated animals suggesting that local delivery of growth factors exerted beneficial effects on the entire heart. Although these findings could be occasionally detected in untreated chronic infarcts, the quantitative estimation clearly indicated that regenerative processes were much more pronounced in MI-GF group both in the infarcted and peri-infarcted area (Figure 9÷12 and Figure 13).

Infarct size, as measured by the amount of myocytes lost 6 weeks after coronary artery ligation, was similar in the two experimental groups. As shown in Figure 14A, more than 4 million myocytes were lost in MI-V and MI-GF hearts. Within the infarcted area, HGF and IGF-1 treatment resulted in the formation of 12.5±5 mm^3 of new myocardium (data not shown) in which $5.1\pm0.1x10^6$ developing myocytes ranging in size from 200 to more than 2500 μm^3 were present (Figure 14B). Conversely, the number of newly formed myocytes in untreated infarcts was unremarkable. Noteworthy, generation of new myocytes increased linearly with the amount of cell lost in GFs treated animals while a similar reparative capacity was not observed in untreated rats (Figure 14C).

These findings strongly suggest that GFs-induced cardiac repair was mediated by a multipotent stem cell population. Indeed, myocardial regeneration was associated with intense activation and translocation of the resident progenitor cell compartment. A nearly 2-fold ($p<0.01$) increase in the density of c-kit^{pos} cells was found in the infarcted, peri-infarcted and remote myocardium of MI-GF hearts in comparison with MI-V (Figure 15), without changes in the distribution of CSC density in the three myocardial regions.

Electrophoretic and immunoblot analysis

To confirm the positive electro-mechanical effects associated with regenerative processes evoked by the intramyocardial injection of GFs, a biochemical quantification of the expression of Cx43 was performed on samples of the infarcted and remote portion of the rat heart. The levels of Cx43 within the infarcted region were negligible in MI-V (Figure 16A). Local GF administration significantly increased the expression of the gap-junctional protein (22-fold vs. MI-V; $p<0.01$; Figure 16B), supporting a better electrical coupling within the scarred partially regenerated myocardium. Similar findings, although of lower magnitude, were observed in the remote spared myocardium (2-fold increase in Cx43 expression levels; $p<0.05$; Figure 16B).

FIGURES and TABLES of EXPERIMENTAL PROTOCOL 1

R-R interval (ms)			
		Baseline	Social stress
Before treatment	SO	170.1 ± 5.3	123.5 ± 2.9 ¥
	MI	172.1 ± 3.5	120.4 ± 1.0 ¥
After treatment	SO-V	182.2 ± 5.8	123.1 ± 2.4 ¥
	MI-V	167.4 ± 4.8 #	122.1 ± 1.2 ¥
	MI- GF	183.4 ± 4.8	125.4 ± 1.8 ¥

SD_{RR} (ms)			
		Baseline	Social stress
Before treatment	SO	11.0 ± 0.4	7.1 ± 0,8 ¥
	MI	10.7 ± 0.6	6.4 ± 0.7 ¥
After treatment	SO-V	10.3 ± 0.7	6.4 ± 0.9 ¥
	MI-V	9.9 ± 0.5	5.2 ± 0.4 ¥
	MI- GF	11.7 ± 0.7	6.5 ± 0.7 ¥

r-MSSD (ms)			
		Baseline	Social stress
Before treatment	SO	3.7 ± 0.3	2.9 ± 0.2 ¥
	MI	4.9 ± 0.3	3.7 ± 0.4 ¥
After treatment	SO-V	4.0 ± 0.4	2.9 ± 0.3 ¥
	MI-V	4.3 ± 0.3	3.3 ± 0.2 ¥
	MI- GF	5 ± 0.4	3.3 ± 0.3 ¥

Table 1: R-R interval and indirect measurements of the autonomic input to the heart. Values are expressed as mean ± S.E.M. ¥ $p<0.01$ different vs. Baseline within each group, # $p<0,05$ different vs. MI-GF.

Figure 1: Ventricular arrhythmic events.

Representative telemetry ECG tracings recorded during stress periods, showing respectively: a normal sinus rhythm (A), and different types of ventricular arrhythmic events (one premature beat in B, one couplet in C, and a brief episode of tachycardia, in D).

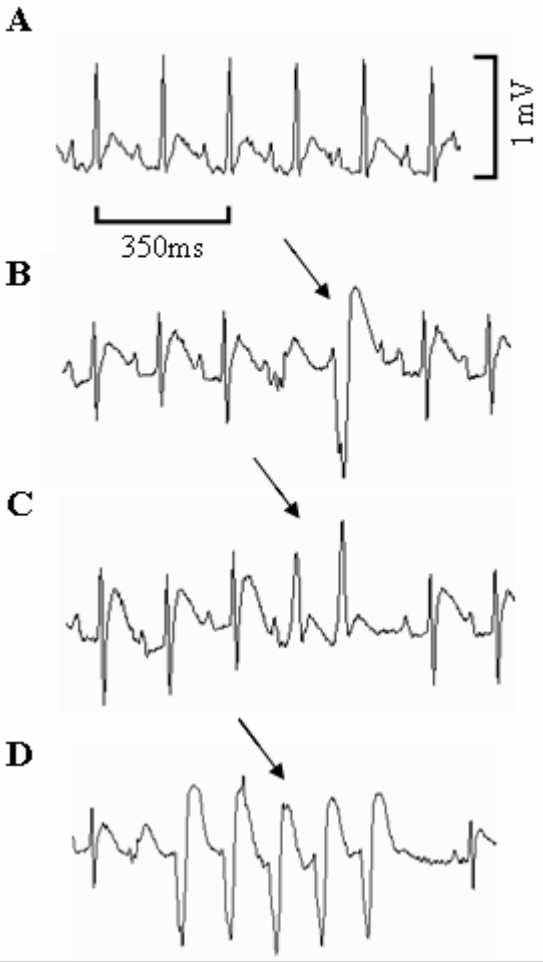

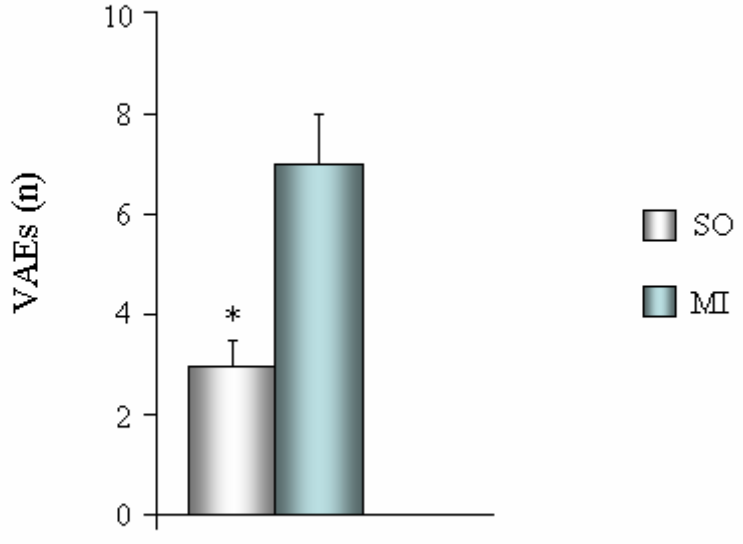

Figure 2. Ventricular arrhythmic events. Mean values ± S.E.M. of stress-induced ventricular arrhythmic events (VAEs) in sham operated (SO) and infarcted (MI) animals, before treatment. * $p<0.05$ vs. MI.

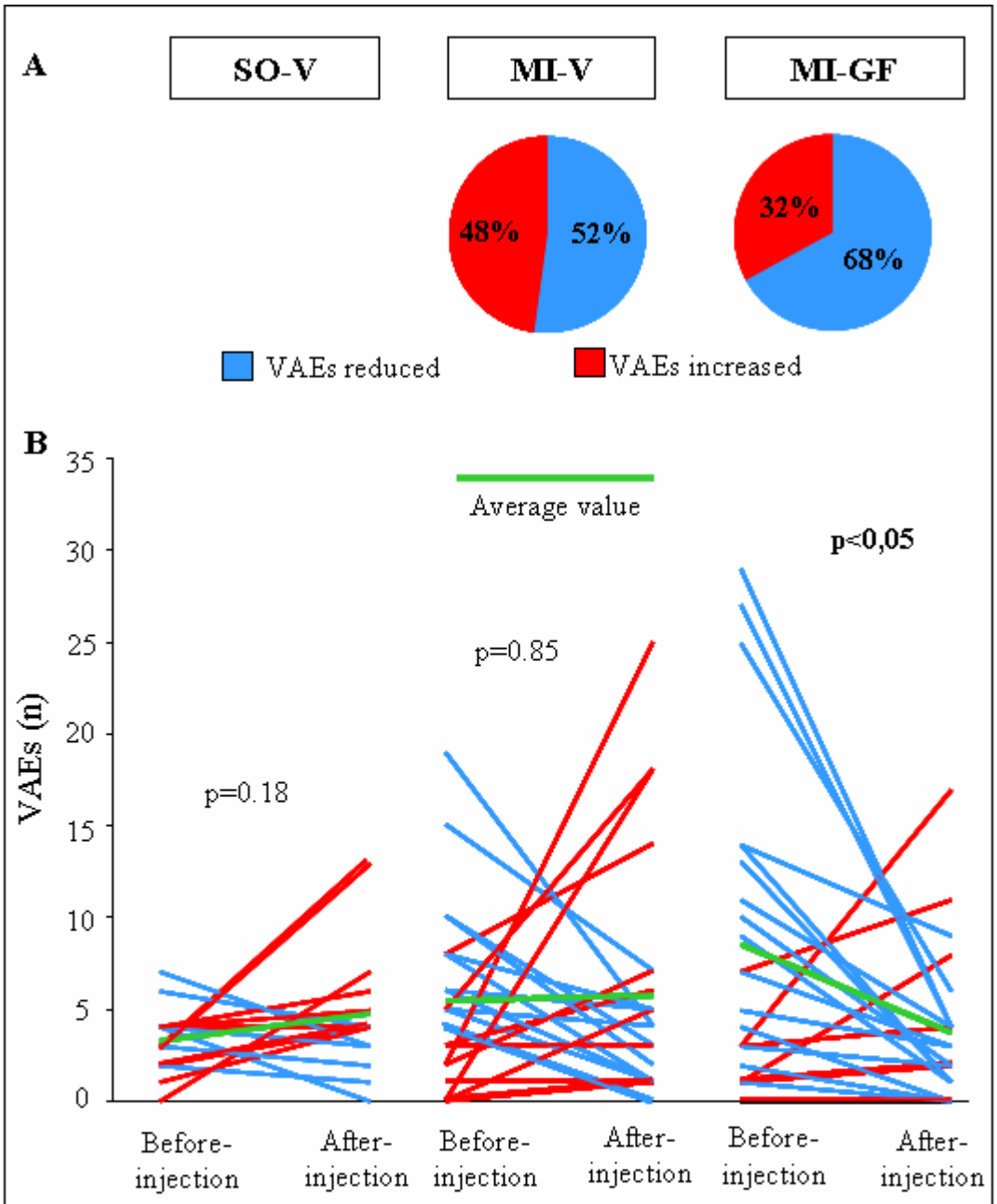

Figure 3. Ventricular arrhythmic events before and after treatment in MI an SO rats. (A) Percentage of rats showing an increase or a decrease in the number of VAEs after treatment, in MI-V and MI-GF groups. (B) In every graph, each line shows the change in the proneness to stress induced VAEs after GFs/V injection, for each animal. On the left the number of VAEs before injection and on the right the number of VAEs after injection. Red lines indicate an increase in VAEs while blue line a decrease. Green line represents the average behavior of the group. VAEs decrease was statistically significant in MI-GF ($p<0.05$).

	Before treatment		
	SO	**MI**	
LVEDD (cm)	0.547 ± 0.021	0.634 ± 0.017	*
LVESD (cm)	0.246 ± 0.014	0.341 ± 0.015	*
LVEDV (ml)	0.397 ± 0.043	0.625 ± 0.044	*
LVESV (ml)	0.042 ± 0.008	0.121 ± 0.015	*
EF (%)	89.49 ± 0.98	82.38 ± 1.18	*
FS (%)	54.79 ± 1.43	46.76 ± 1.25	*

Table 2: **Echocardiographic measurements.** Data are presented as mean ± S.E.M. Abbreviation: SO, sham-operated group; MI, infarcted animals; LVEDD, left-ventricular end-diastolic diameter; LVESD, left ventricular end-systolic diameter; LVEDV, left ventricular end-diastolic volume; LVESV, left ventricular end-systolic volume; EF, ejection fraction; FS, fractional shortening. * $p<0.05$ vs. SO.

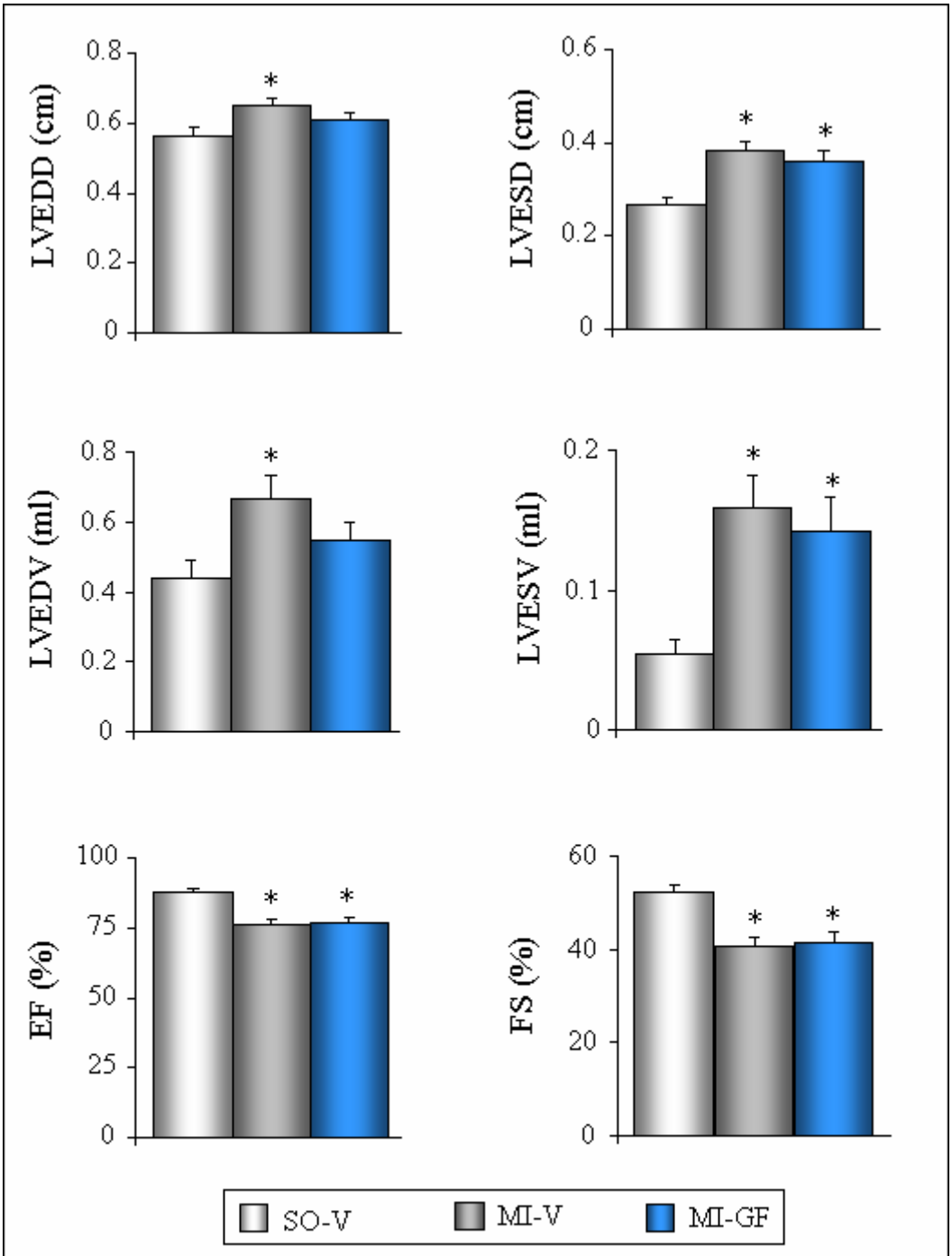

Figure 4. Echocardiographic measurements. LVEDD, left-ventricular end-diastolic diameter; LVESD, left ventricular end-systolic diameter; LVEDV, left ventricular end-diastolic volume; LVESV, left ventricular end-systolic volume; EF, ejection fraction; FS, fractional shortening in the different experimental groups. Data are presented as mean ± S.E.M. * $p<0.05$ vs. SO-V.

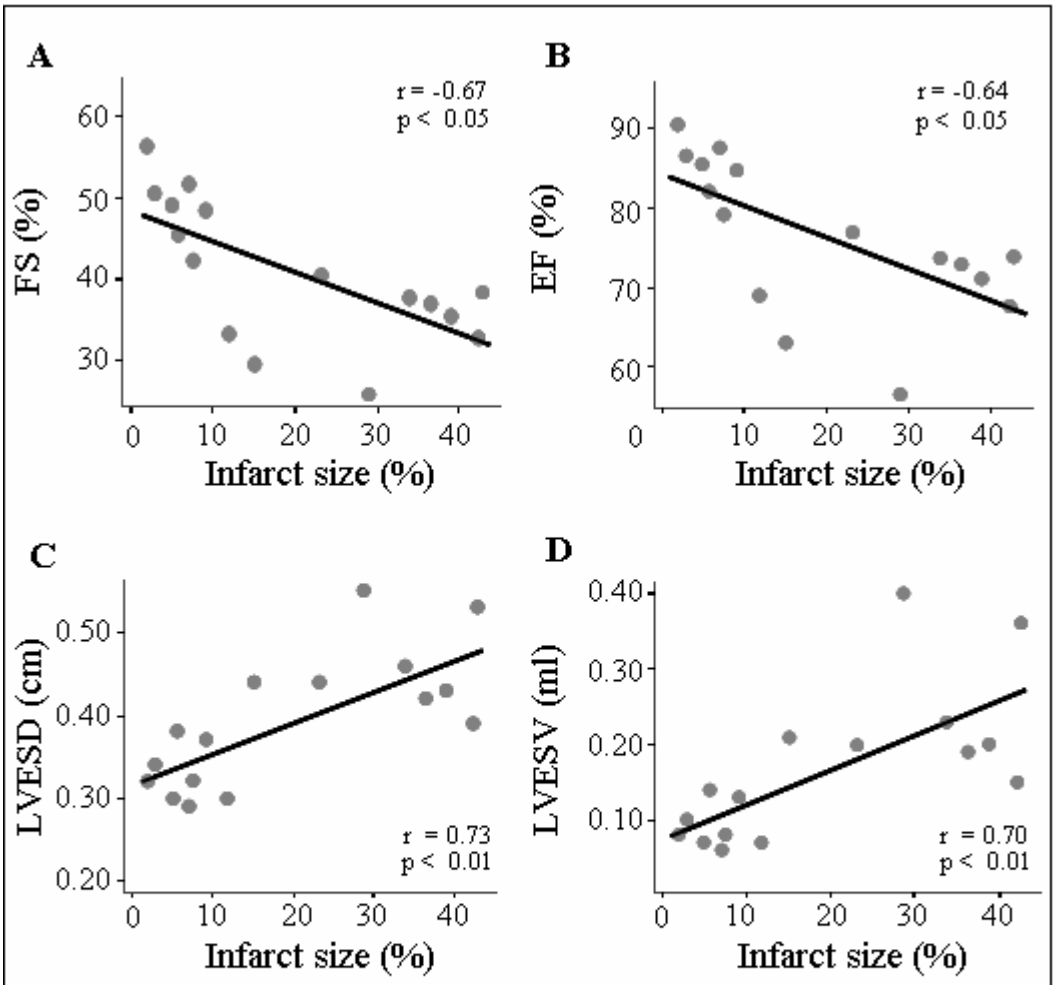

Figure 5. Echocardiographic measurements: correlations in MI-V rats. Significant negative correlations between infarct size (%) and: (A) fractional shortening (FS) and (B) ejection fraction (EF). Significant positive correlations between infarct size (%) and: (C) left ventricular end-systolic diameter (LVESD) and (D) left ventricular end-systolic volume (LVESV).

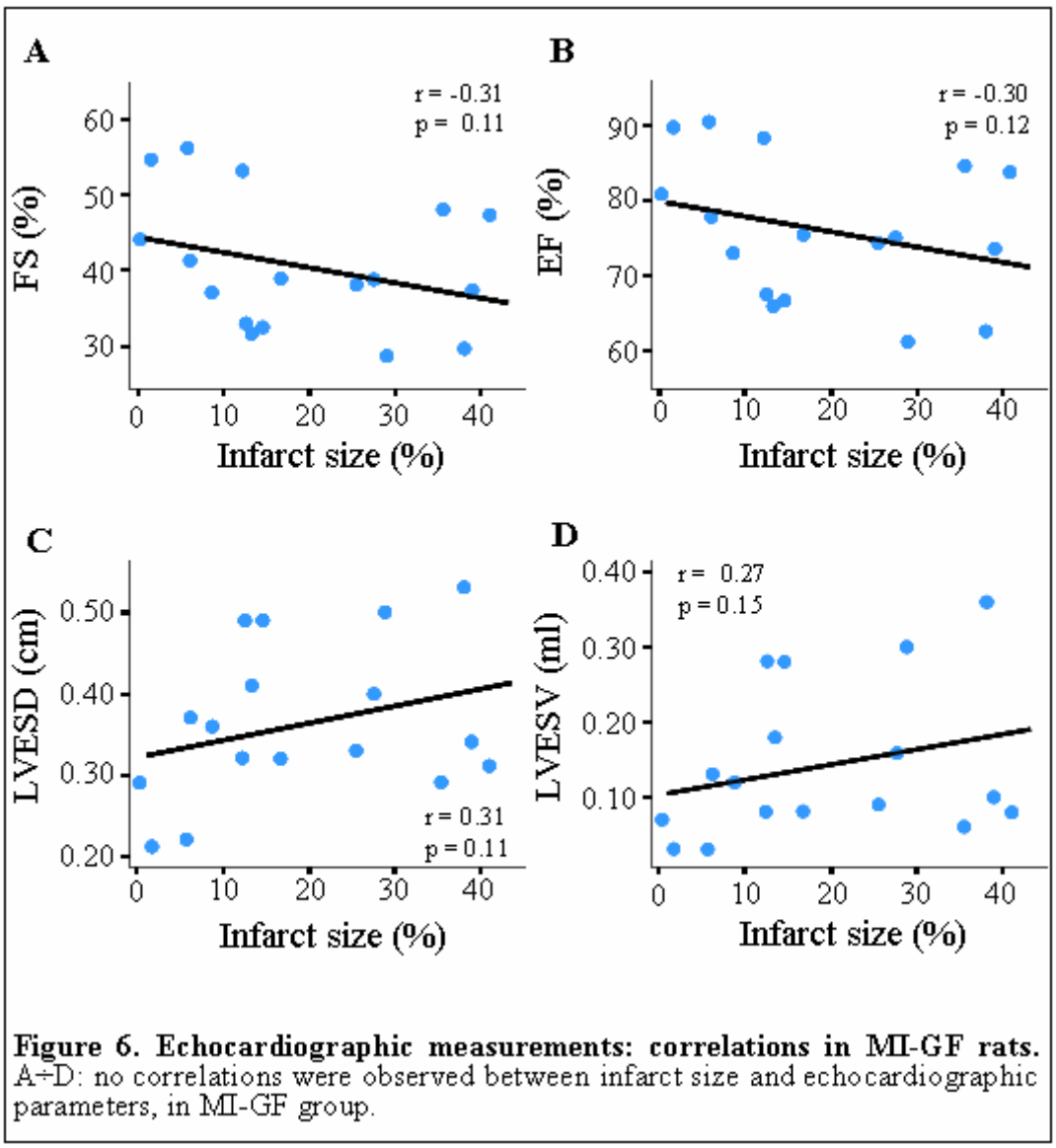

Figure 6. Echocardiographic measurements: correlations in MI-GF rats. A÷D: no correlations were observed between infarct size and echocardiographic parameters, in MI-GF group.

	SO-V	MI-V		MI-GF	
LVSP (mmHg)	121.8 ± 2.17	110.3 ± 3.02	*	107.6 ± 2.72	*
+dP/dt (mmHg/s)	9351 ± 391	8232.6 ± 367	*	7530.7 ± 319	*
-dP/dt (mmHg/s)	-5852.7 ± 174	-4806.2 ± 270	*	-4546.9 ± 243	*

Table 3. Hemodynamic studies. LVSP, left ventricular systolic pressure, maximal rate of ventricular pressure rise (+dP/dt) and decline (-dP/dt), measured in the three experimental groups. Values are reported as mean ± S.E.M. * $p<0.05$ vs. SO-V.

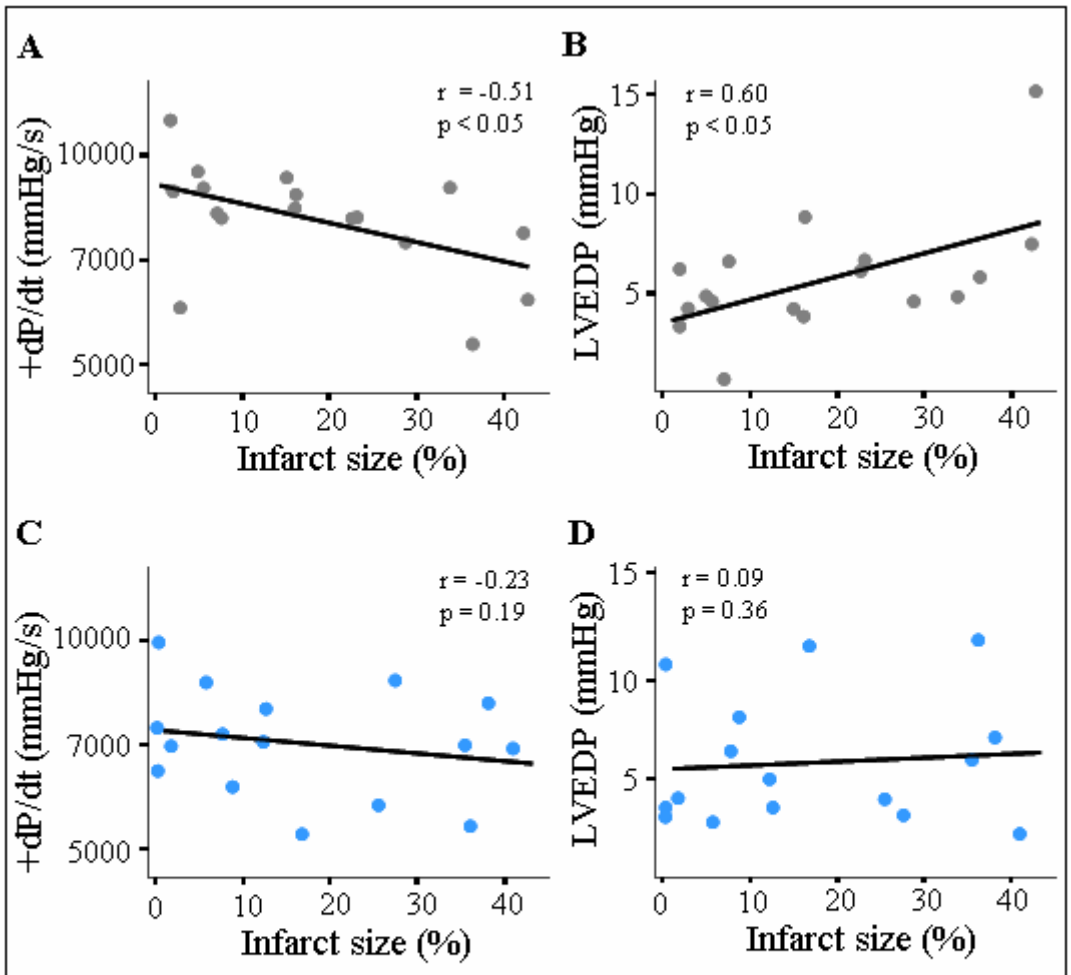

Figure 7. Hemodynamic studies: correlations. Significant correlations between infarct size (%) and: (A) maximal rate of ventricular pressure rise (+dP/dt) and (B) left ventricular end diastolic pressure (LVEDP), in MI-V animals. Conversely, MI-GF group did not show any significant correlations (C and D).

	SO-V	MI-V	MI-GF
LVW (mg)	899 ± 57	1109 ± 37 *	1093 ± 18 *
LVW/BW (mg/g)	1.9 ± 0.12	2.5 ± 0.08 *	2.5 ± 0.05 *
LVmass (mm^3)	849 ± 53	1046 ± 35 *	1031 ± 17
LVchamber volume (mm^3)	204 ± 11	429 ± 28 *	347 ± 21 * #
LVmass/chambre volume	4.2 ± 0.1	2.4 ± 0.1 *	3.1 ± 0.2 * #
LV wall thickness (mm)	2,4 ± 0.1	2 ± 0.06 *	2.2 ± 0.06

Table 4. Gross cardiac characteristics. LVW, left ventricular weight; BW, body weight. Values are reported as mean ± S.E.M. * $p<0.01$ vs. SO-V; # $p<0.05$ significant differences between MI-V and MI-GF.

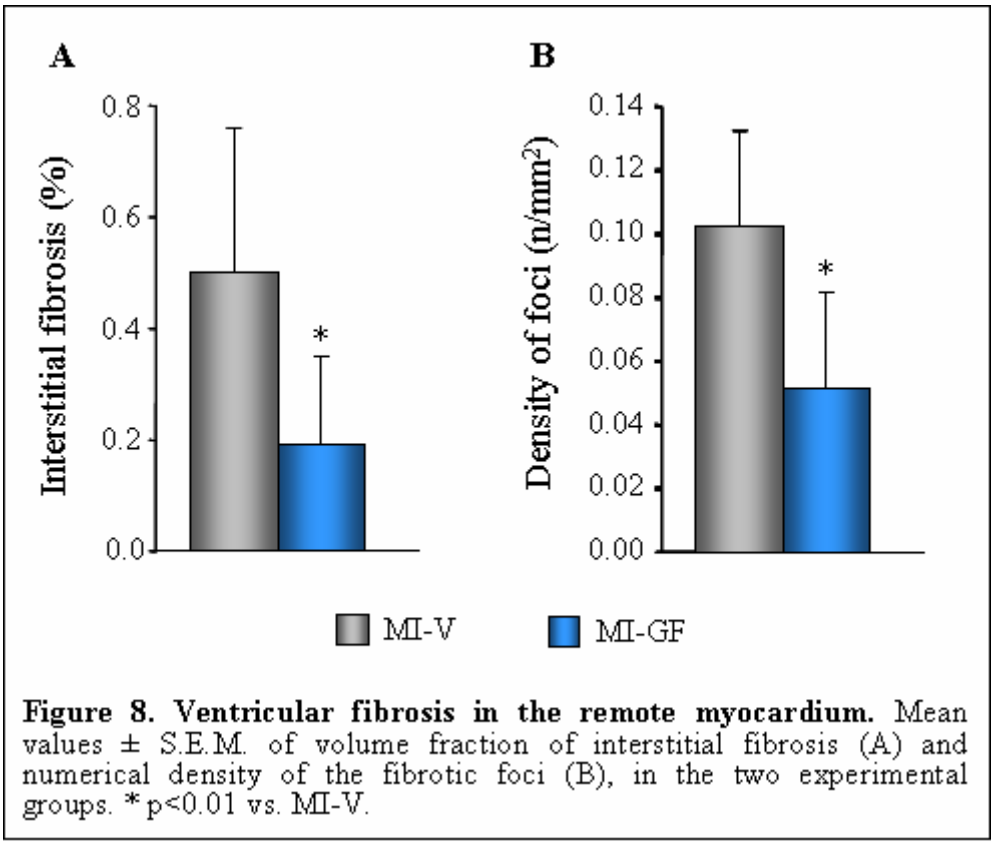

Figure 8. Ventricular fibrosis in the remote myocardium. Mean values ± S.E.M. of volume fraction of interstitial fibrosis (A) and numerical density of the fibrotic foci (B), in the two experimental groups. * $p<0.01$ vs. MI-V.

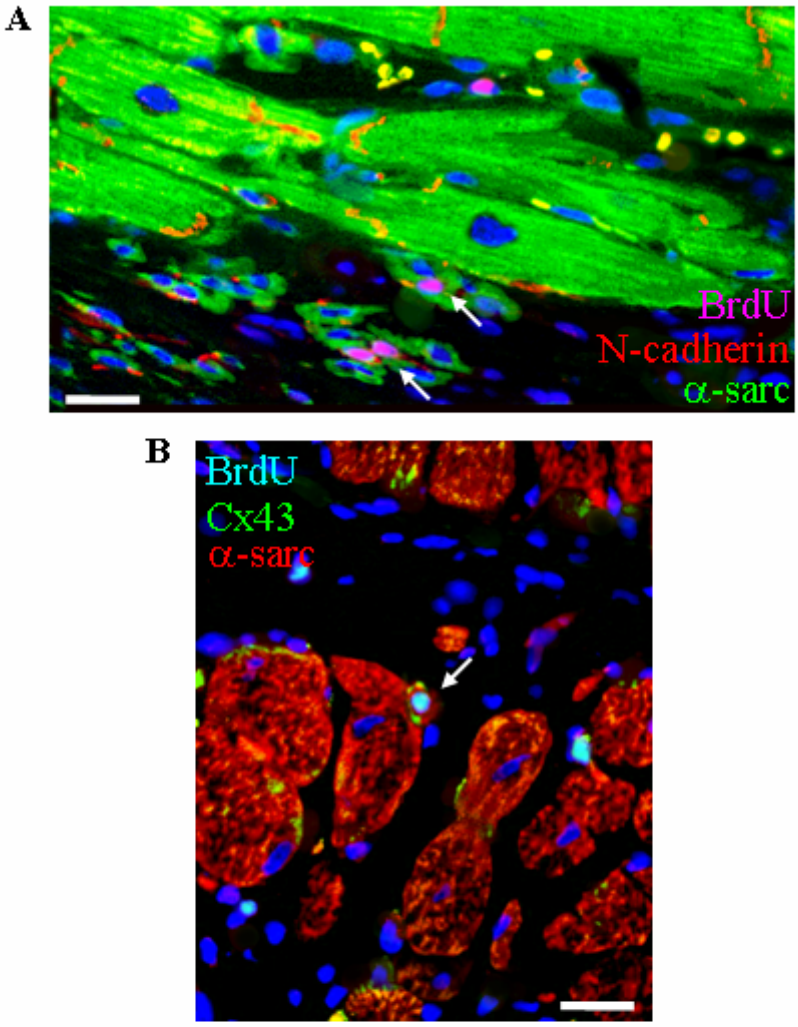

Figure 9. Immunohistochemical study. Formation of functionally competent myocardium. Panel A: the arrows indicate small, $BrdU^{pos}$ (magenta fluorescence) cardiomyocytes (α-sarc actin positive: green fluorescence) connected by N-cadherin (red fluorescence) in the infarcted area, and one newly formed myocyte mechanically connected with the spared myocardium in the peri-infarcted region. Panel B: a small, $BrdU^{pos}$ (light blue fluorescence) and α-sarc actin positive (red fluorescence) cardiomyocyte connected by Cx43 (green fluorescence) with spared myocytes is indicated by the arrow, in the peri-infarcted area. The nuclei (blue fluorescence) are stained with bisbenzimide.

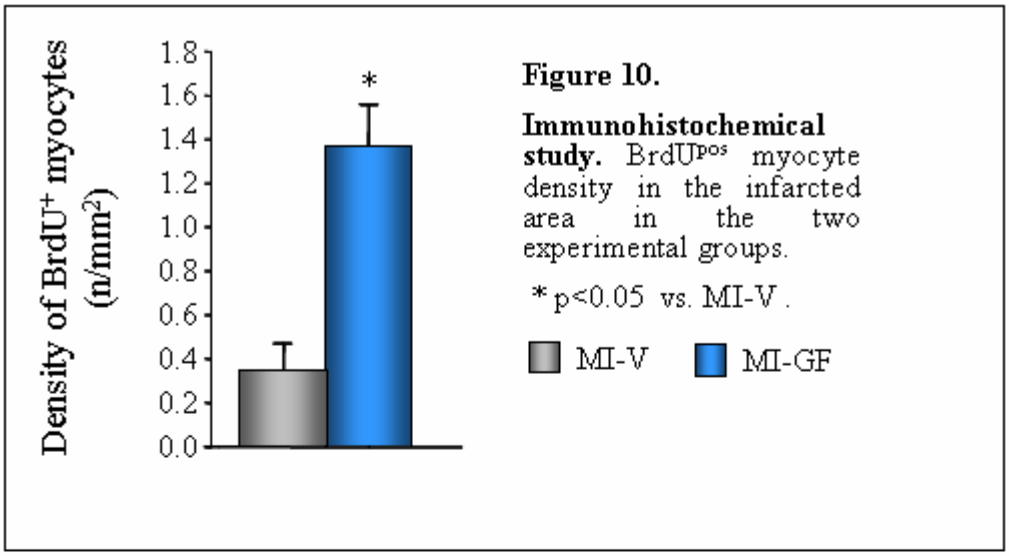

Figure 10.

Immunohistochemical study. $BrdU^{pos}$ myocyte density in the infarcted area in the two experimental groups.

* $p<0.05$ vs. MI-V.

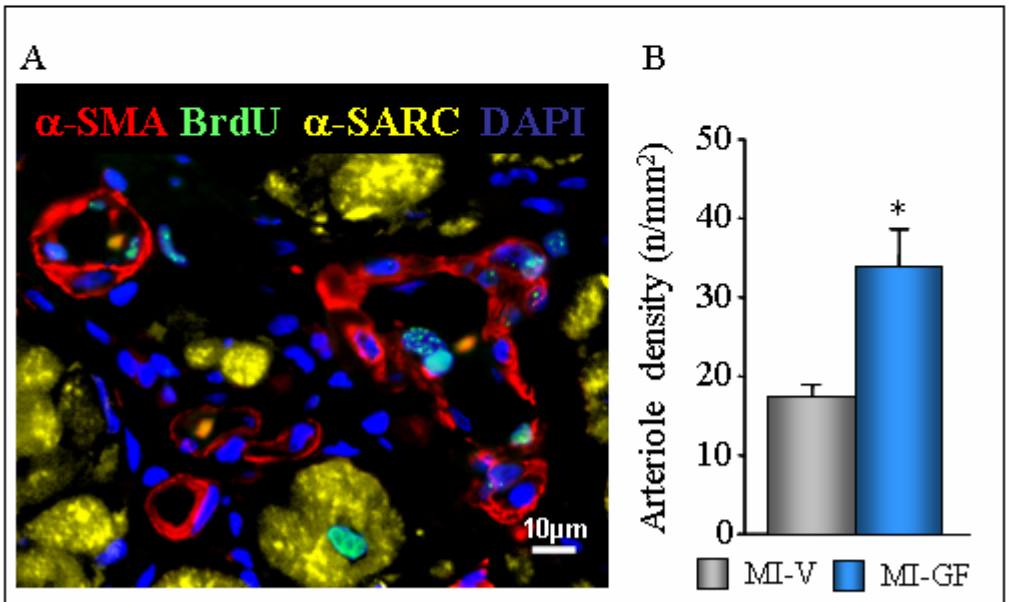

Figure 11. Immunohistochemical study. (A) Newly formed arterioles are recognized by double staining for BrdU (green fluorescence) and by the red fluorescence of α-SMA. The blue fluorescence of DAPI corresponds to nuclei. α-sarcomeric actin: yellow. (B) Arteriole density in the infarcted area of the two experimental groups. * $p<0.05$ vs. MI-V.

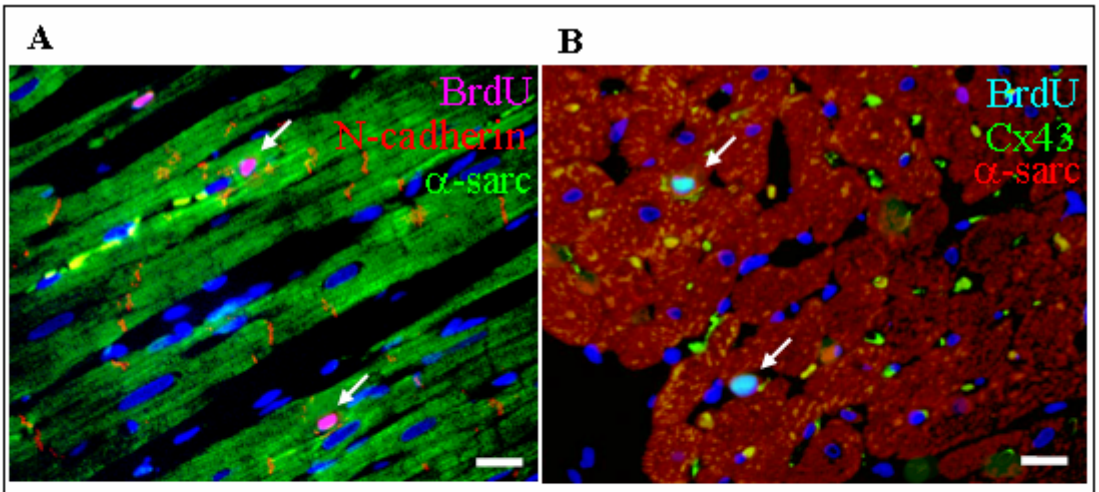

Figure 12. Immunohistochemical study. Formation of functionally competent myocardium in the remote area. Panel A: small, BrdU^{pos} (magenta fluorescence) and α-sarc actin positive (green fluorescence) cardiomyocytes connected by N-cadherin (red fluorescence) with surrounding myocytes. Panel B: small, BrdU^{pos} (light blue fluorescence) and α-sarc actin positive (red fluorescence) cardiomyocytes connected by Cx43 (green fluorescence) with bordering cells. The blue fluorescence of bisbenzimide corresponds to nuclei.

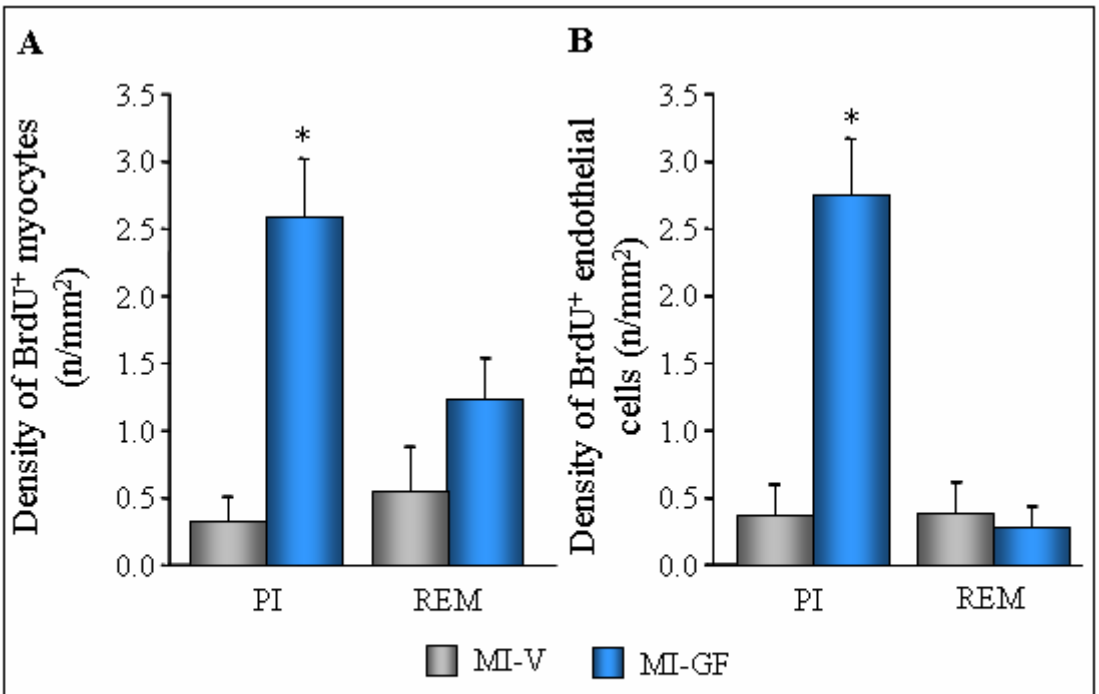

Figure 13. Immunohistochemical study. BrdU^{pos} myocyte density (A) and BrdU^{pos} endothelial cell density (B) in the peri-infarcted area (PI) and in the remote zone (REM), in the two experimental groups. * $p<0.01$ vs. MI-V .

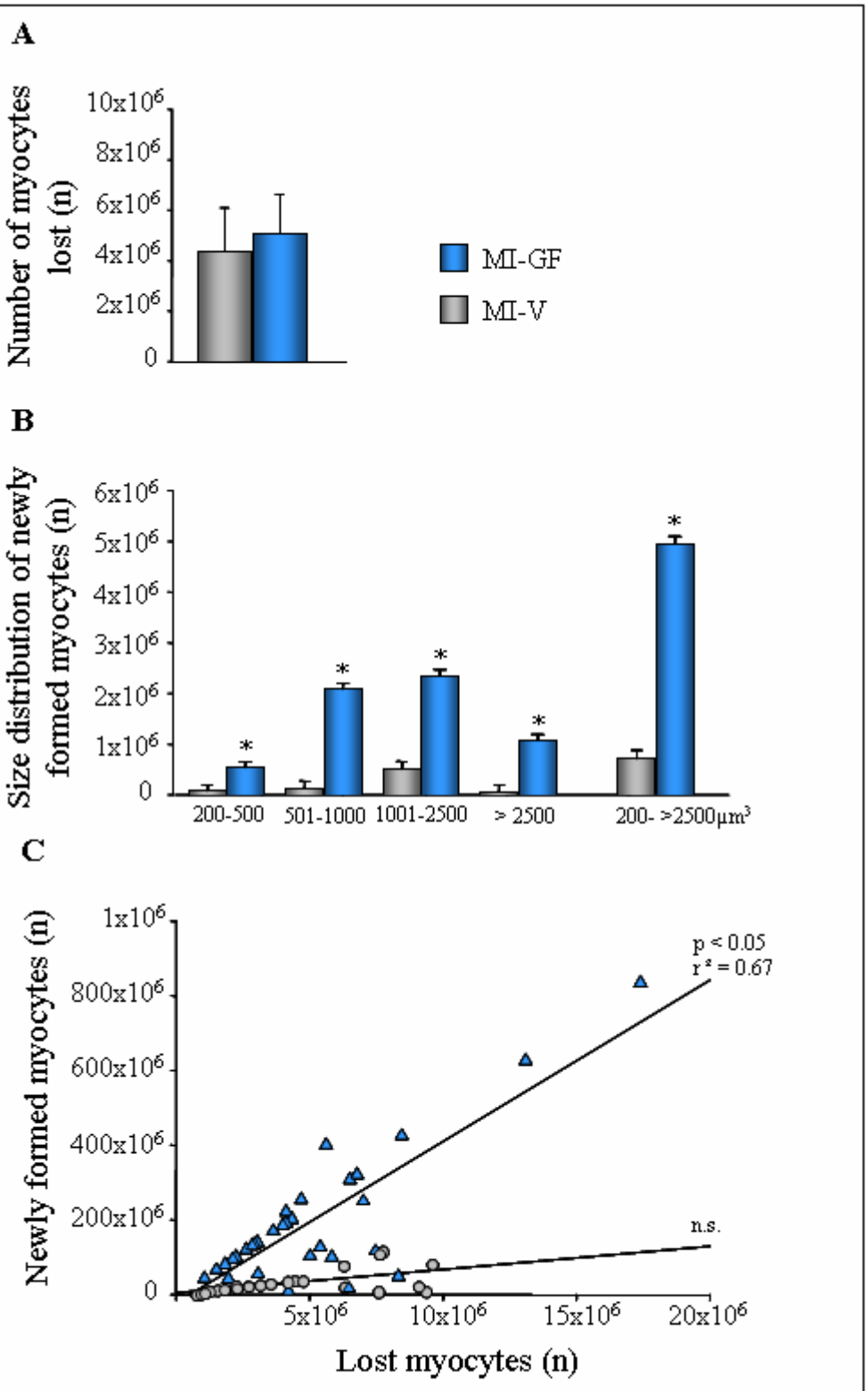

Figure 14. (A) Number of myocytes lost in the two experimental groups. (B) Size distribution of newly formed myocytes in MI-V and MI-GF. (C) Correlations between the number of newly formed myocytes and lost myocytes in the two groups. * $p<0.05$ vs. MI-V.

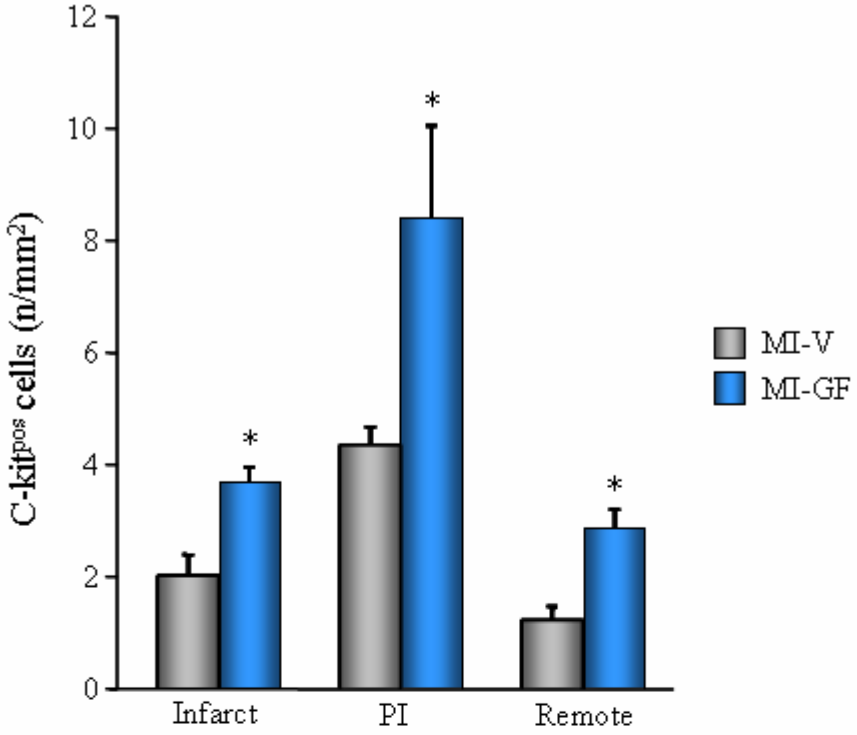

Figure 15. Number of c-kit^{pos} cells in the infarcted, peri-infarcted (PI) and remote areas in the two experimental groups. * $p<0.01$ vs. MI-V.

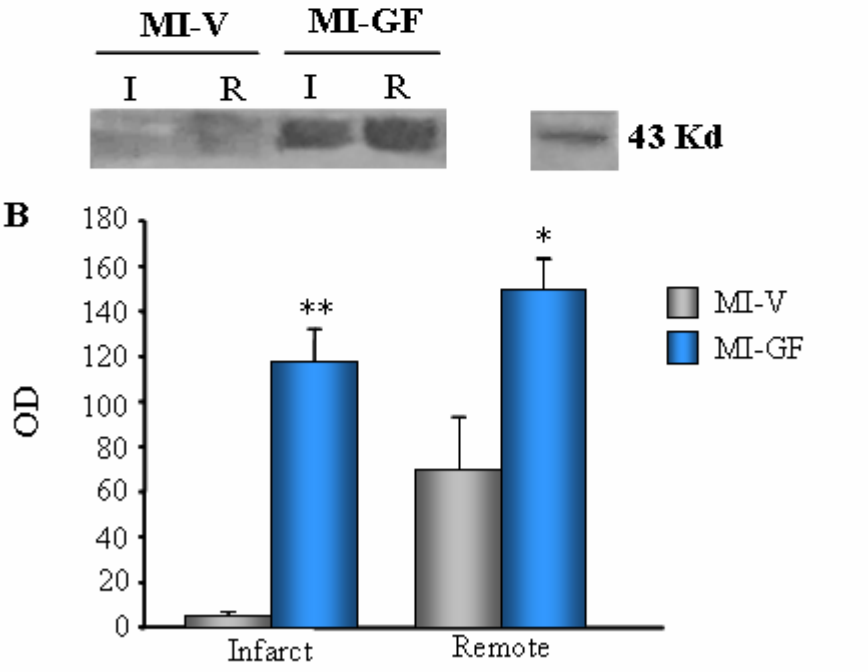

Figure 16. Cx43 expression. (A) Western blot analysis of Cx43 in MI-V and MI-GF rats in infarcted and remote areas; (B) Corresponding quantification by optical density is reported by mean values ± S.E.M. ** $p<0.01$, * $p<0.05$ vs. MI-V.

RESULTS of EXPERIMENTAL PROTOCOL 2

IN VIVO STUDIES

Telemetry ECG recordings

R-R interval and indirect measurements of the autonomic input to the heart. In all groups, before and after treatment, social stress exposure induced a significant decrease in R-R interval (Table 1) associated with a parallel decrease of heart rate variability indices, as expected as a consequence of the sympathetic activation. In addition, both treatments provoked a slight prolongation of R-R interval. No significant differences were found among groups, with the exception of lower average values of SD_{RR} observed before treatment in MI as compared with SO (Table 1).

Proneness to arrhythmias. In all groups, ventricular arrhythmic events (VAEs) consisted of isolated premature beats, some couplets and occasionally more complex pattern especially found in infarcted rats (Figure 1). Arrhythmia vulnerability was evaluated as number of ventricular arrhythmic events (VAEs) during stress periods. Before CPCs, CPCs+GFs or V injection, stress VAEs were negligible in SO rats (3,5±0.4) and were increased about three fold in infarcted rats ($p<0,01$; Figure 2). In SO animals VAEs remained unchanged after CPCs or CPCs+GFs treatment (Figure 4). In infarcted animals, the injections of saline or CPCs alone were ineffective while the treatment with CPCs in combination with growth factors significantly reduced VAEs (by three-fold in 100% of MI-cells+GF rats; $p<0.02$) (Figure 4A, B). Thus, the addition of GFs to CPCs is essential to reduce the proneness to arrhythmias triggered by sympathetic stimulation in conscious animals with chronic myocardial infarction.

Hemodynamic studies

A worsening of left ventricular mechanical function was observed in MI-saline as compared with SO-cells and SO-cells+GF, as indicated by the significant reduction in the maximal rate of ventricular pressure rise (+dP/dt) and the increase in left ventricular end-diastolic pressure (LVEDP). Both MI-treated infarcts exhibited an improvement of the two parameters, suggesting a partial recovery of ventricular contractile efficiency (Figure 5A, B).

In addition, the deterioration of ventricular contractility and the degree of LV chamber dilation (as measured by +dP/dt and LVEDP) were correlated with infarct size only in MI-saline group (Figure 6A, B). Conversely, the two relationships were lost in MI-cells+GF (Figure 6C, D) and MI-cells (Figure 6E, F) groups, confirming that both treatments renders the alterations of LV structure and mechanical performance independent of the size of damaged myocardium.

POST MORTEM STUDIES

Cardiac Structure

We tested whether the beneficial effects of both regenerative treatments on the electro-mechanical properties of the infarcted heart had a structural-anatomical counterpart.

Gross Cardiac Anatomy. Myocardial infarcts without treatment resulted in a 42% increase in left ventricular chamber volume and 35% decrease in ventricular mass/chamber volume ratio (Figure 7A, B).

Treatment with CPCs or CPCs+GF resulted in a quite complete recovery of LV structure. Indeed, ventricular dilation and the change in ventricular mass/chamber volume ratio, representing the major anatomical determinants of heart failure, were reduced by approximately 30% (Figure 7A, B), approaching the average values observed in SO groups.

Immunohistochemical analysis of myocardial regeneration

Homing of injected QDots-loaded CPCs to the infarcted heart was documented in unstained left ventricular sections by a band (dotted line area) containing yellow fluorescent dots corresponding to QD585 excitation by UV light (Figure 8A).

Engraftment of CPCs and formation of functionally competent myocardium was detected by the presence of small, α-sarcomeric actin positive cardiomyocytes

connected by gap junctions (Figure 8B).

Since QDots methodology does not allow a simultaneous quantification of cell engraftment and differentiation, the fate of injected EGFP-CPCs was documented by anti-GFP immunostaining (Figure 9). By this analysis, a significant increase in the EGFP positive cells density was observed, from the remote myocardium to the infarcted area ($p<0.05$; Figure 9 and Figure 10). However, the addition of GFs to CPCs resulted in a significant higher number of EGFP positive cells within the infarcted myocardium as compared with MI-cells ($p<0.02$; Figure 10).

Newly formed cardiomyocytes derived from the differentiation of the injected EGFP-CPCs were observed in treated infarcted hearts (Figure 11A). Moreover, vasculogenesis in the infarcted area, was demonstrated by the presence of EGFP positive arterioles as a result of the differentiation of CPCs into α-smooth muscle actin positive cells (Figure 11B).

Quantification of these regenerative processes showed that in the infarcted area the number of arterioles was three-fold increased in both treated groups as compared to MI-saline ($p<0.02$; Figure 12), while the density of EGFP positive cardiomyocytes was two-fold higher in MI-cells+GF than in MI-cells group ($p<0.05$; Figure 13).

Importantly, GFs added to CPCs increased by 6-folds the number of spared fully mature cardiomyocytes within the infarcted myocardium (Figure 14).

Finally, the effects of the injection of CPCs or CPCs+GF on cell proliferation was determined by BrdU incorporation into the DNA of myocardial cells. Compared to untreated rats, a significant increase in the total number of cycling $BrdU^{pos}$ cells was measured in the infarcted and spared myocardium of both treated groups (Figure 15). However, compared to CPCs, the addition of GFs to CPCs increased by 1.5-folds, 1.8-folds and 1.5-folds the number of $BrdU^{pos}$ cells in the remote, peri-infarcted and infarcted areas, respectively (Figure 15). Similar results were obtained when the analysis of cycling cells was restricted to cardiomyocytes. As shown in figure 16, both treatments exerted a positive effect on cardiomyocyte proliferation in the myocardium proximal and remote to infarction. This phenomenon was more pronounced in MI-cells+GF group although the difference did not reach the statistical significance.

In order to determine whether cycling myocytes were generated by the injected CPCs or by activation and differentiation of a resident progenitor cell population

mediated by paracrine factors, simultaneous staining for EGFP, BrdU and sarcomeric filaments is under investigation.

FIGURES and TABLES of EXPERIMENTAL PROTOCOL 2

R-R interval (ms)			
		Baseline	Social stress
Before treatment	SO	166.9 ± 3.6	124.7 ± 1.3 ¥
	MI	173 ± 2.7	124.45 ± 1.05 ¥
After treatment	SO-cells	180 ± 5.4	129.9 ± 2.9 ¥
	SO-cells+GF	184 ± 4.7	126.9 ± 2.1 ¥
	MI-cells	187 ± 3.6	128.2 ± 1.5 ¥
	MI-cells+GF	187.6 ± 4.2	131.5 ± 1.9 ¥
	MI-saline	171.5 ± 6	124.1 ± 1.5 ¥

SD_{RR} (ms)			
		Baseline	Social stress
Before treatment	SO	12.4 ± 0.61	7.8 ± 0.66 ¥
	MI	11.2 ± 0.53	6 ± 0.36 * ¥
After treatment	SO-cells	12.38 ± 0.46	8.26 ± 1 ¥
	SO-cells+GF	12.26 ± 0.4	6.7 ± 0.63 ¥
	MI-cells	11.03 ± 0.8	6.72 ± 0.82 ¥
	MI-cells+GF	11.6 ± 1	5.38 ± 0.56 ¥
	MI-saline	9.85 ± 0.7	5.06 ± 0.87 ¥

r-MSSD (ms)			
		Baseline	Social stress
Before treatment	SO	3.94 ± 0.19	3.04 ± 0.17 ¥
	MI	4.75 ± 0.27	3.25 ± 0.19 ¥
After treatment	SO-cells	4.1 ± 0.29	3.62 ± 0.52 ¥
	SO-cells+GF	4.02 ± 0.28	3.59 ± 0.48 ¥
	MI-cells	4.59 ± 0.45	2.85 ± 0.2 ¥
	MI-cells+GF	5.06 ± 0.24	3.51 ± 0.36 ¥
	MI-saline	4.97 ± 0.57	3.41 ± 0.29 ¥

Table 1: R-R interval and indirect measurements of the autonomic input to the heart. Values are expressed as mean ± S.E.M. ¥ $p<0.01$ different vs. Baseline within each group.* $p<0.05$ different vs. SO.

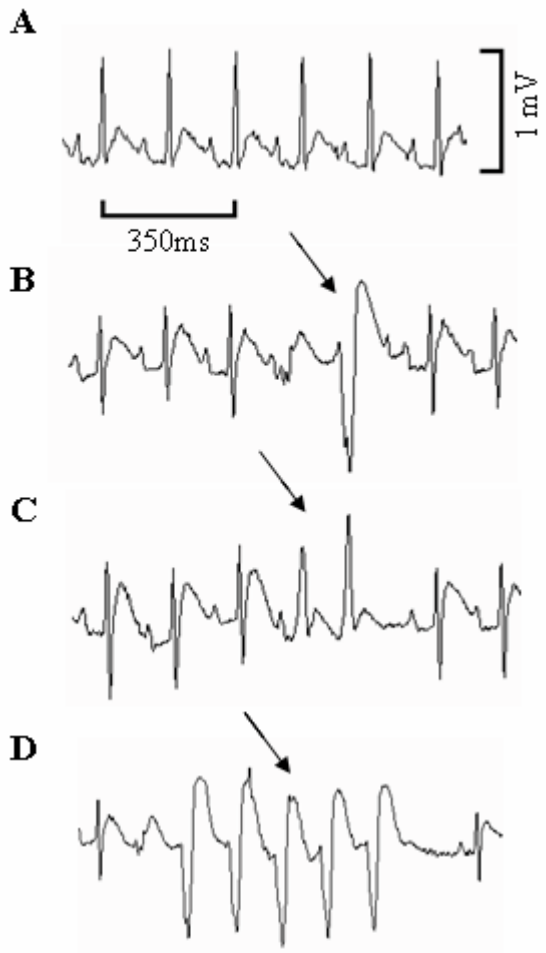

Figure 1: Ventricular arrhythmic events. Representative telemetry ECG tracings recorded during stress periods, showing respectively: a normal sinus rhythm (A), and different types of ventricular arrhythmic events (one premature beat in B, one couplet in C, and a brief episode of tachycardia, in D).

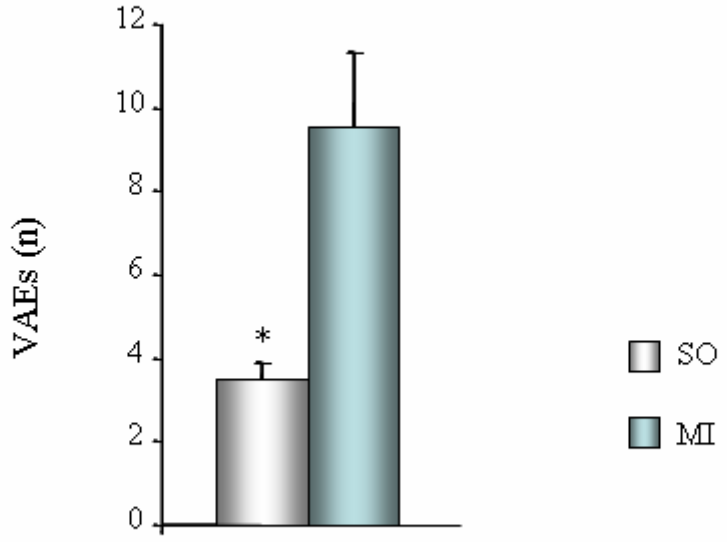

Figure 2. Ventricular arrhythmic events. Mean values ± S.E.M. of stress-induced ventricular arrhythmic events (VAEs) in sham operated (SO) and infarcted (MI) animals, before treatment. * $p<0.05$ vs. MI.

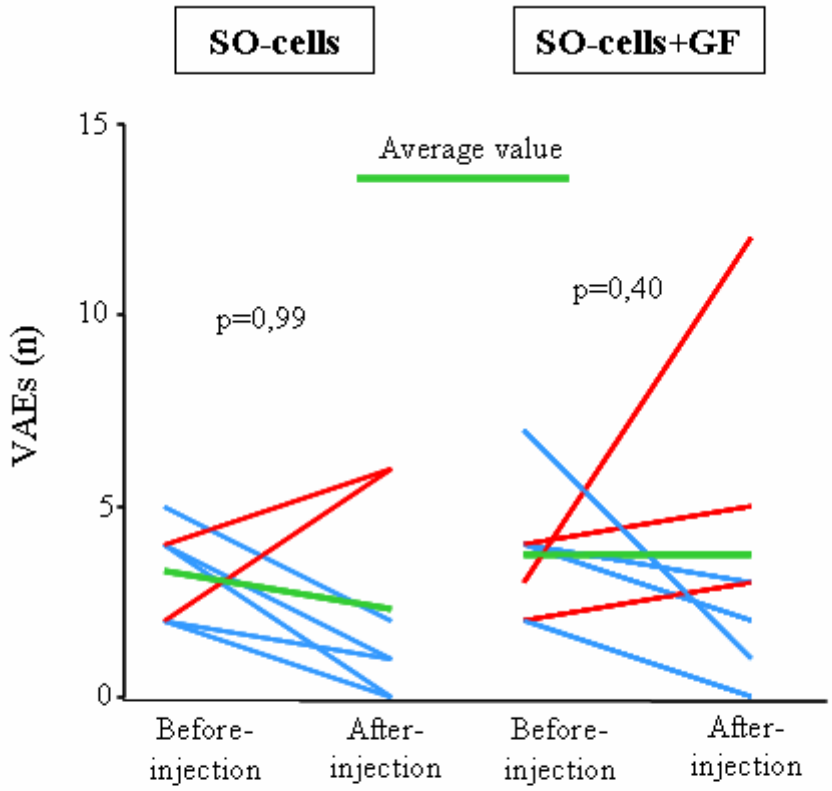

Figure 3. Ventricular arrhythmic events before and after treatment in SO rats. In every graph, each line shows the change in the proneness to stress induced VAEs after cells/cells+GFs injection, for every SO-animal. On the left the number of VAEs before injection and on the right the number of VAEs after injection. Red lines indicate an increase in VAEs while blue line a decrease. Green line represents the average behavior of the group. Both treatments did not induce any significant change in arrhythmia vulnerability, in SO animals.

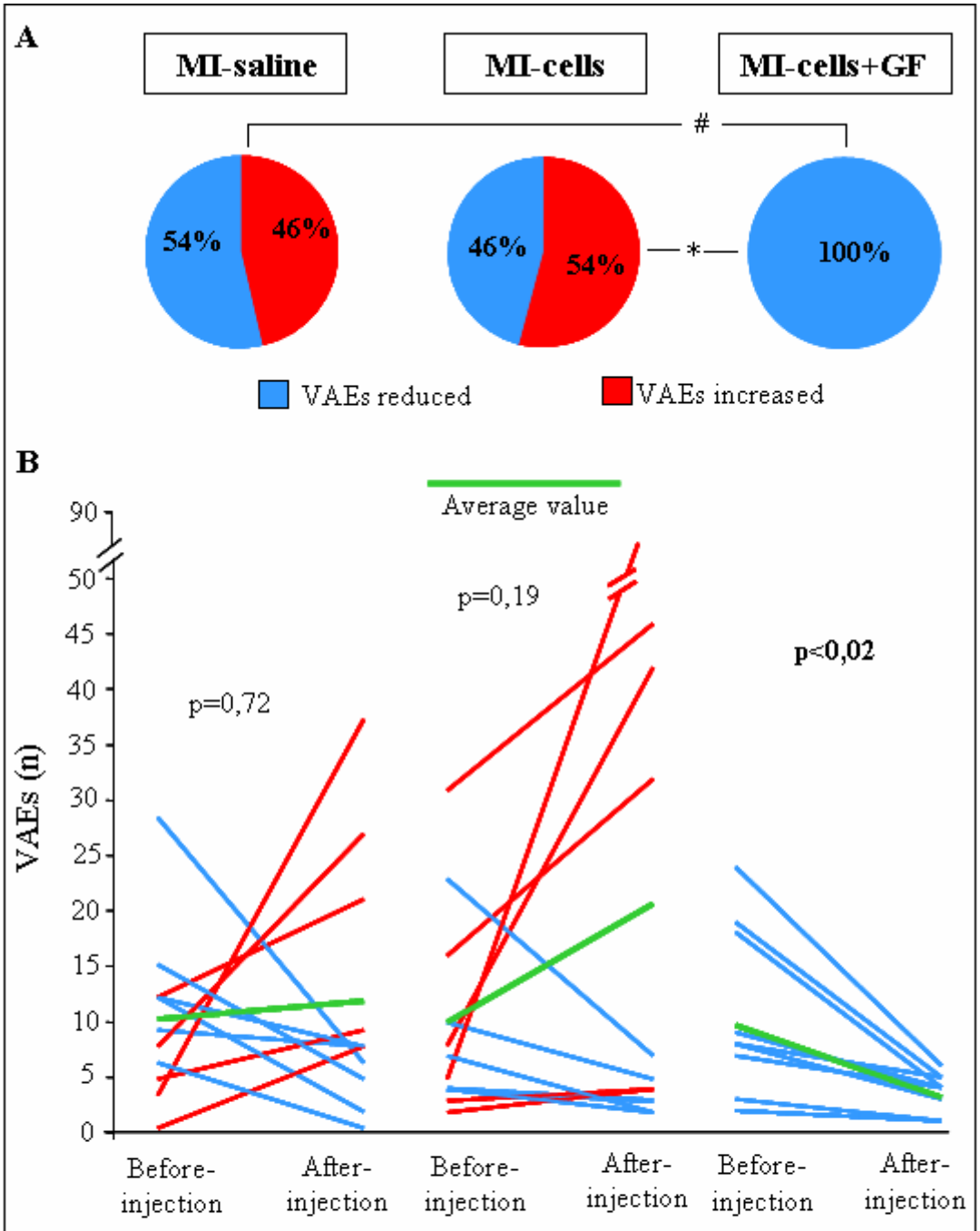

Figure 4. Ventricular arrhythmic events before and after treatment in MI rats. (A) Percentage of rats showing an increase or a decrease in the number of VAEs after treatment. # $p<0.05$ statistically significant differences between MI-saline and MI-cells+GF and * $p<0.05$ significant differences between MI-cells and MI-cells+GF. (B) In every graph, each line shows the change in the proneness to stress induced VAEs after saline/cells/cells+GFs injection, for each animal. On the left the number of VAEs before injection and on the right the number of VAEs after injection. Red lines indicate an increase in VAEs while blue line a decrease. Green line represents the average behavior of the group. VAEs decrease was statistically significant in MI-cells+GF ($p<0.02$).

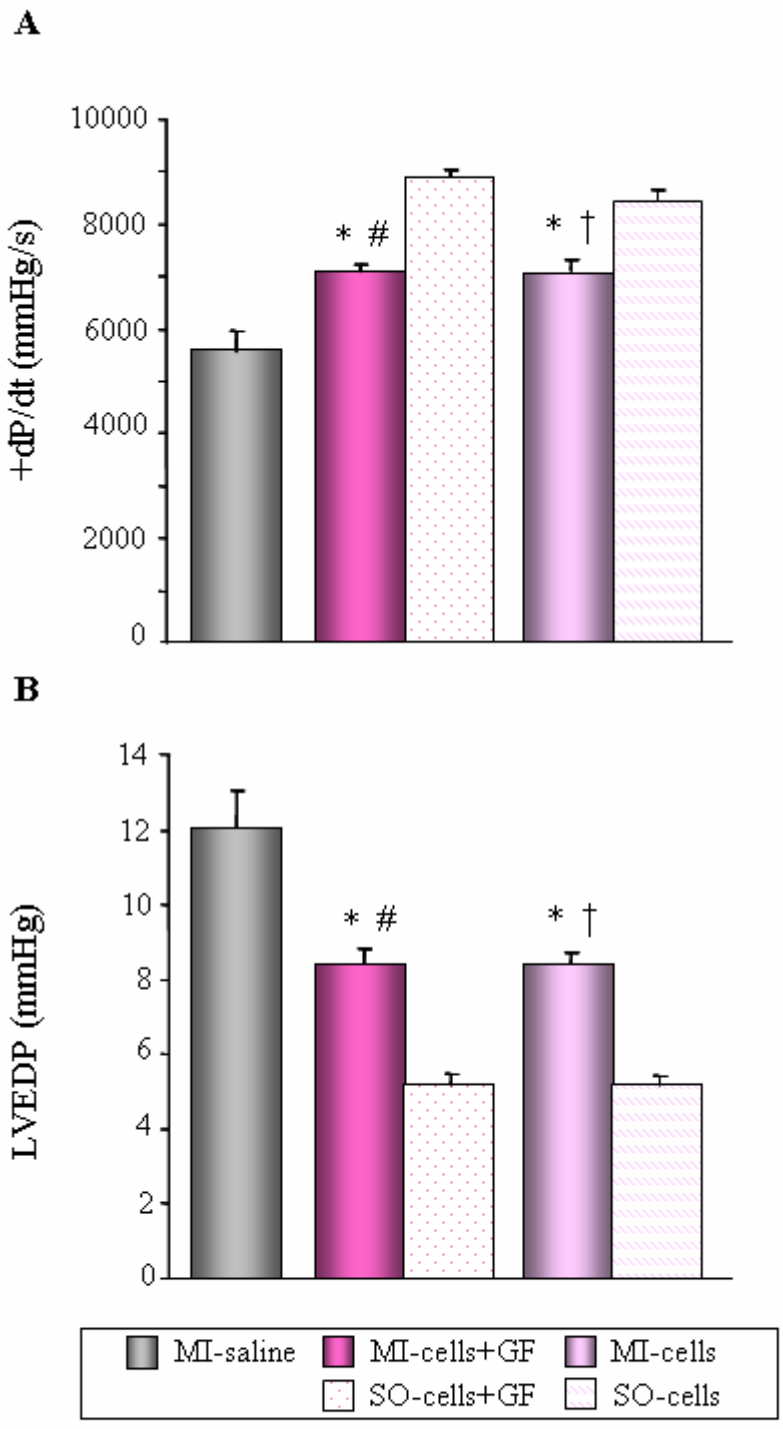

Figure 5. Hemodynamic measurements. Mean values ± S.E.M. of maximal rate of ventricular pressure rise (+dP/dt; A) and left ventricular end-diastolic pressure (LVEDP, B) in the experimental groups. * $p<0.05$ vs. MI-saline, # $p<0.05$ vs. SO-cells+GF, † $p<0.05$ vs. SO-cells.

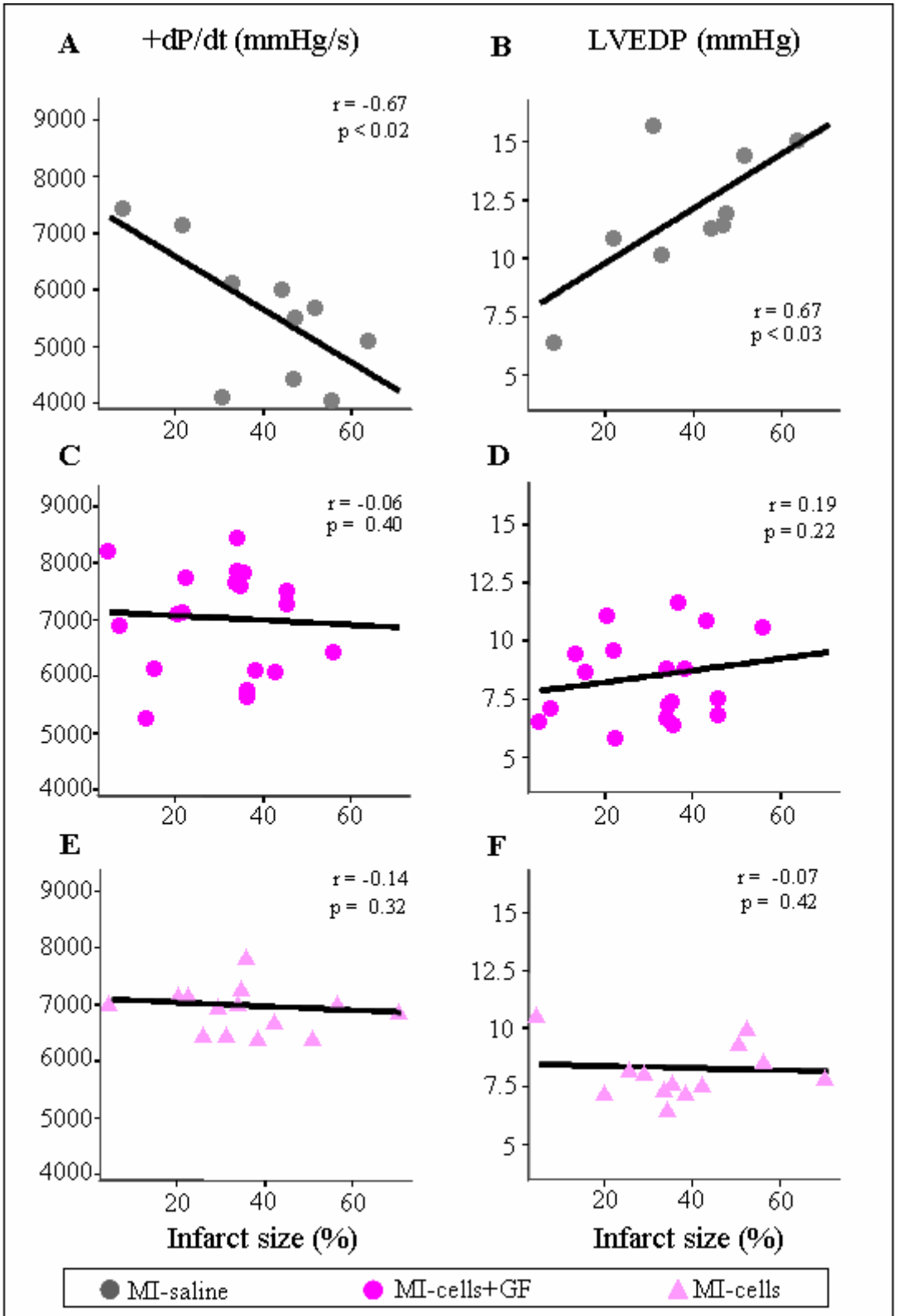

Figure 6. Hemodynamic measurements: correlations. Linear correlations between infarct size (%) and maximal rate of ventricular pressure rise (+dP/dt, A) and left ventricular end-diastolic pressure (LVEDP, B), in MI-saline rats. No correlations were observed between infarct size and hemodynamic parameters in both MI-cells+GF (C and D) and in MI-cells group (E and F).

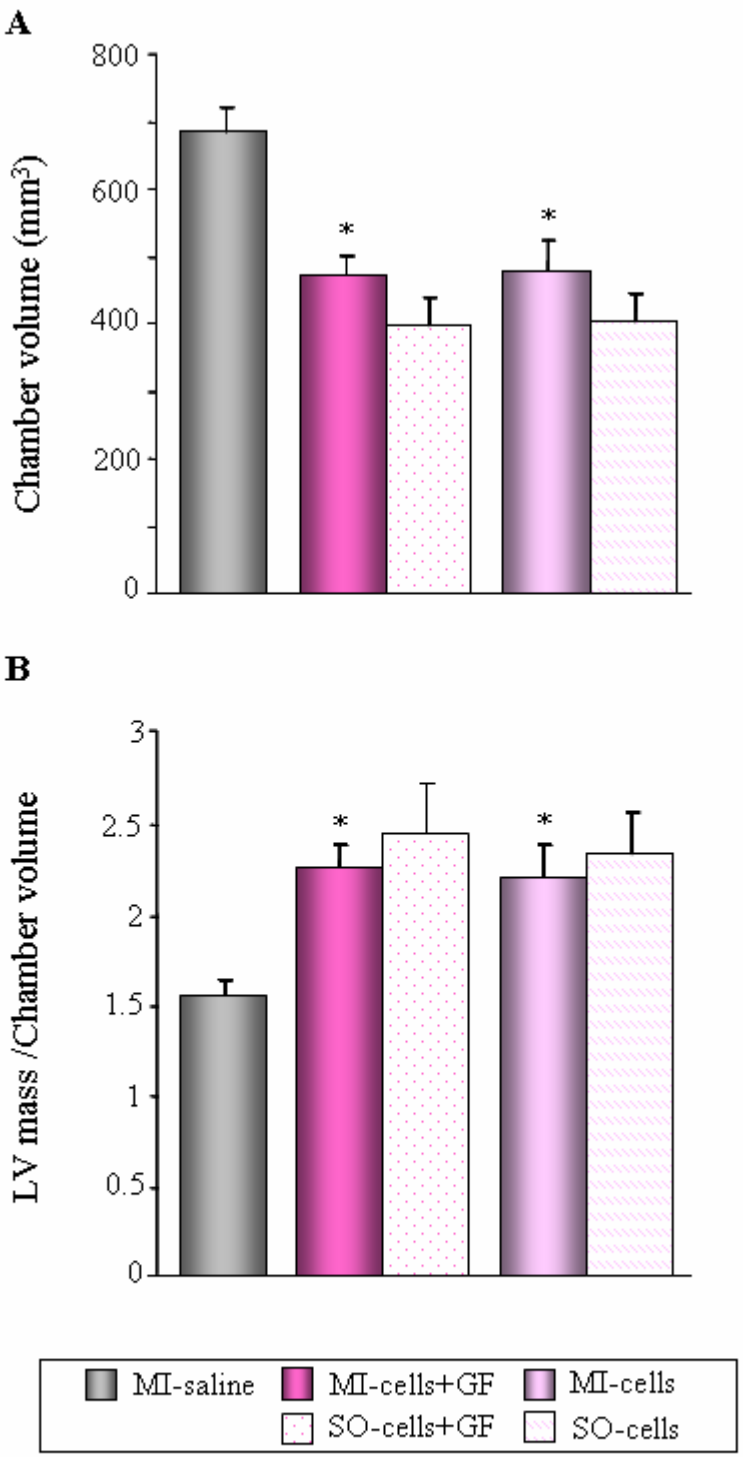

Figure 7. Gross cardiac characteristics. Left ventricular chamber volume (A) and left ventricular mass to chamber volume ratio (B) in all experimental groups. Data are presented as mean ± S.E.M. * $p<0.05$ vs. MI-saline.

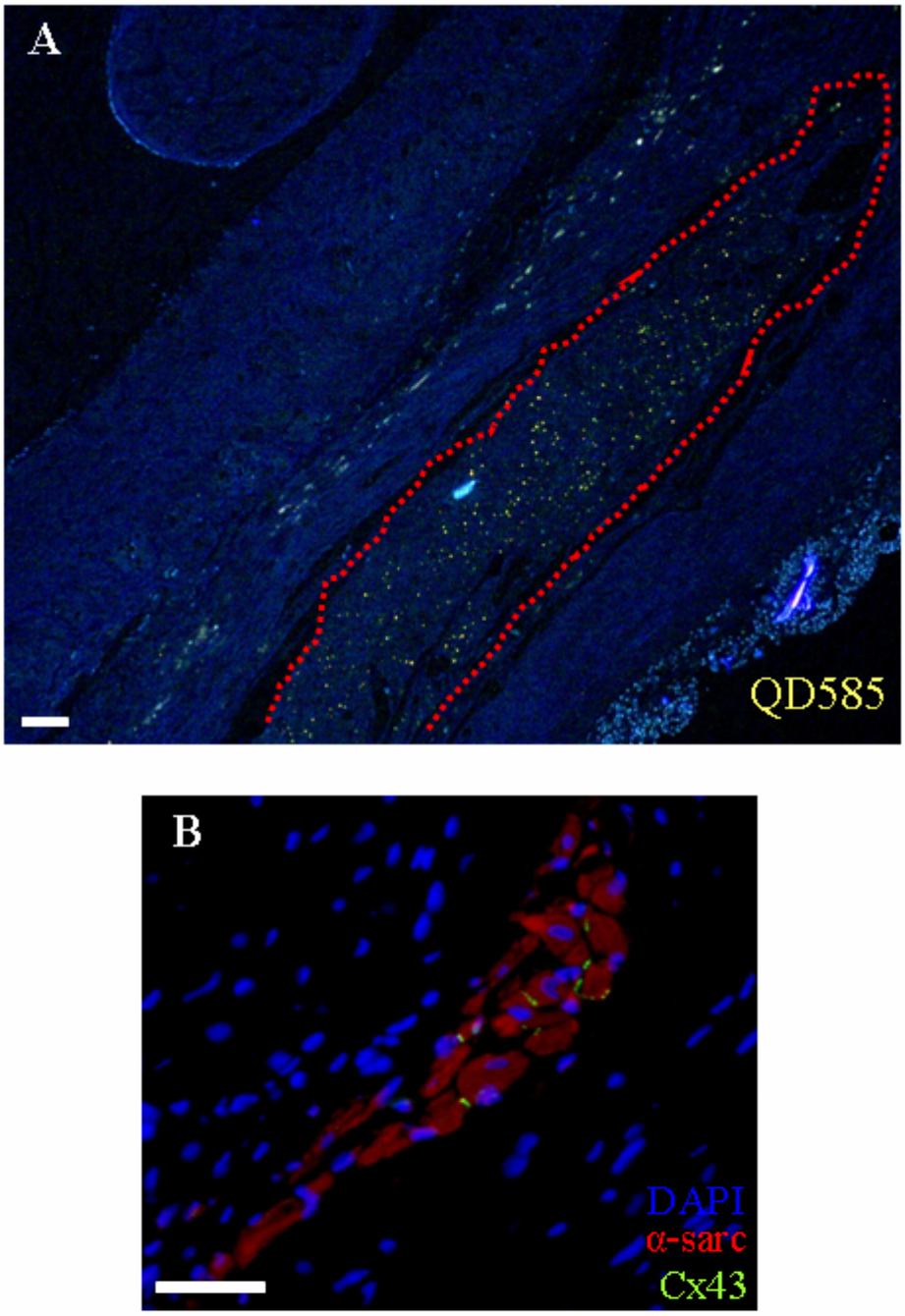

Figure 8. Homing and engraftment of CPCs. Panel A: homing of CPCs to the infarcted heart of cells+GFs treated rat is documented by a band (dotted line area) of yellow fluorescent QD585 in unstained left ventricular sections excited by UV light. Panel B: engraftment of CPCs and formation of functionally competent myocardium is shown by the presence of small, α-sarcomeric actin positive (red fluorescence) cardiomyocytes connected by gap junctions (connexin43, green fluorescence). The blue fluorescence of DAPI corresponds to nuclei.

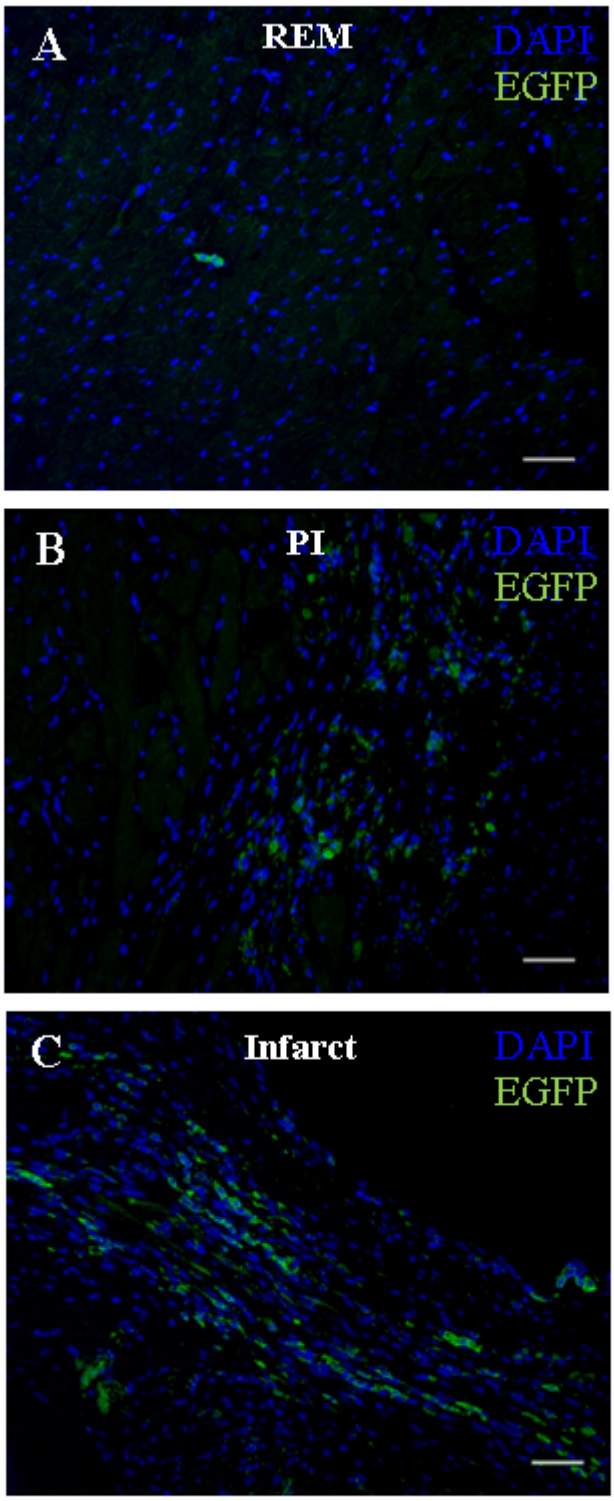

Figure 9. Immunohistochemical study. Homing of the injected CPCs in the remote (REM, Panel A), peri-infarcted (PI, Panel B), and infarcted (Infarct, Panel C) areas. Green fluorescence corresponds to EGFP and the blue fluorescence of DAPI corresponds to nuclei.

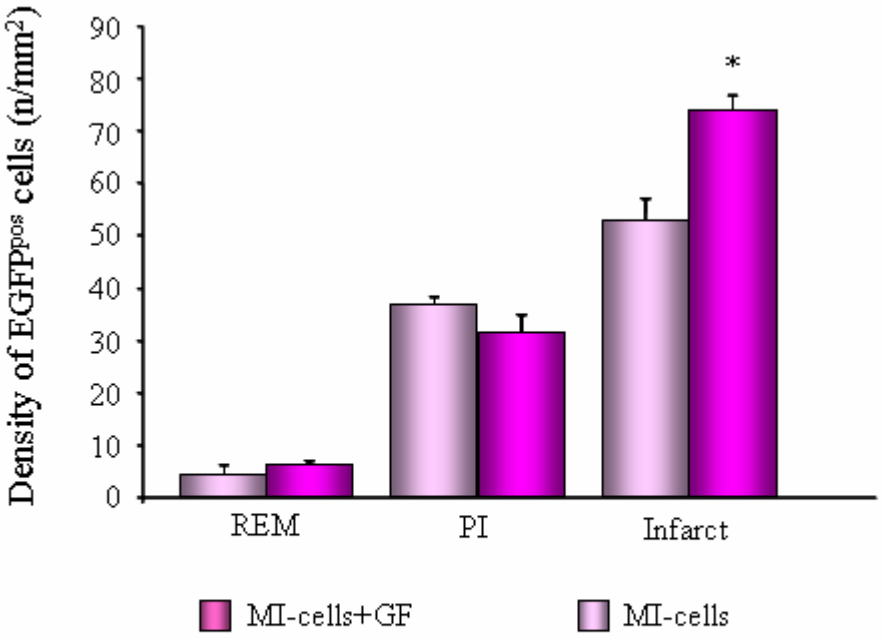

Figure 10. Immunohistochemical study. Number of EGFP positive cells in the remote (REM), peri-infarcted (PI) and infarcted (Infarct) areas, in the two experimental groups. Data are presented as mean ± S.E.M. * $p<0.02$ vs. MI-cells.

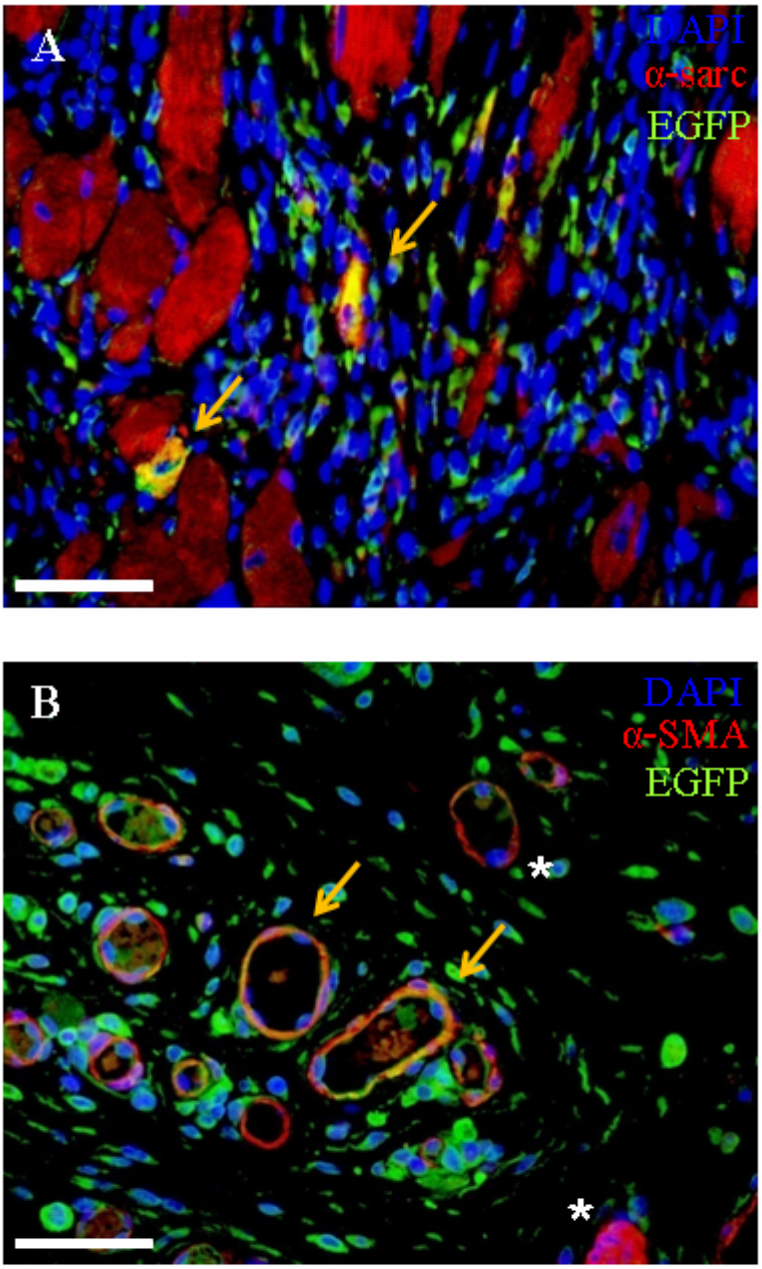

Figure 11. Immunohistochemical study. Myocardial regeneration in the peri-infarcted myocardium of the rat heart injected with CPCs+GFs is shown in Panel A. Green fluorescence corresponds to EGFP while yellow fluorescence documents that EGFP-CPCs generate α-sarcomeric actin (red fluorescence) positive mature cardiomyocytes (arrows). Spared muscle fibers surround the damaged area. Panel B: vasculogenesis in the infarcted area is illustrated by the presence of yellow fluorescent arterioles (arrows) as a result of the differentiation of EGFP-CPCs into α-smooth muscle actin (red fluorescence) positive cells. * indicates rat resident arterioles. The blue fluorescence of DAPI corresponds to nuclei.

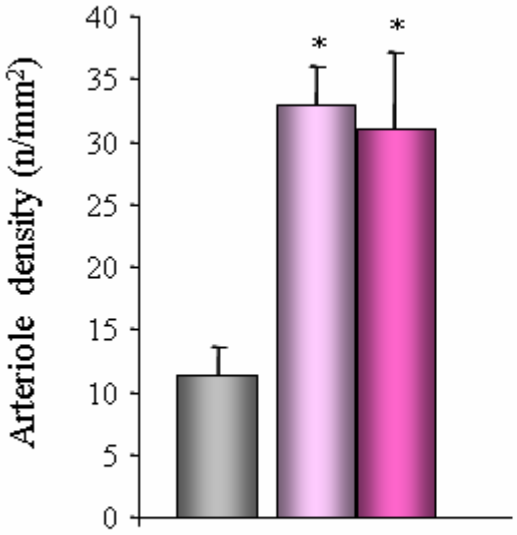

Figure 12.

Immunohistochemical study. Arteriole density in the infarcted area of the three experimental groups, after treatment. Data are presented as mean ± S.E.M.

* $p<0.02$ vs. MI-saline

MI-saline
MI-cells
MI-cells+GF

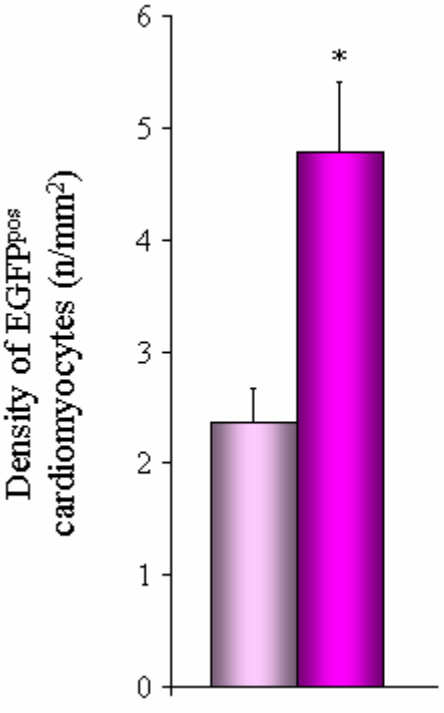

Figure 13.

Immunohistochemical study. Number of EGFP positive cardiomyocytes in the infarcted area in the two experimental groups. Data are presented as mean ± S.E.M.

* $p<0.05$ vs. MI-cells.

MI-cells
MI-cells+GF

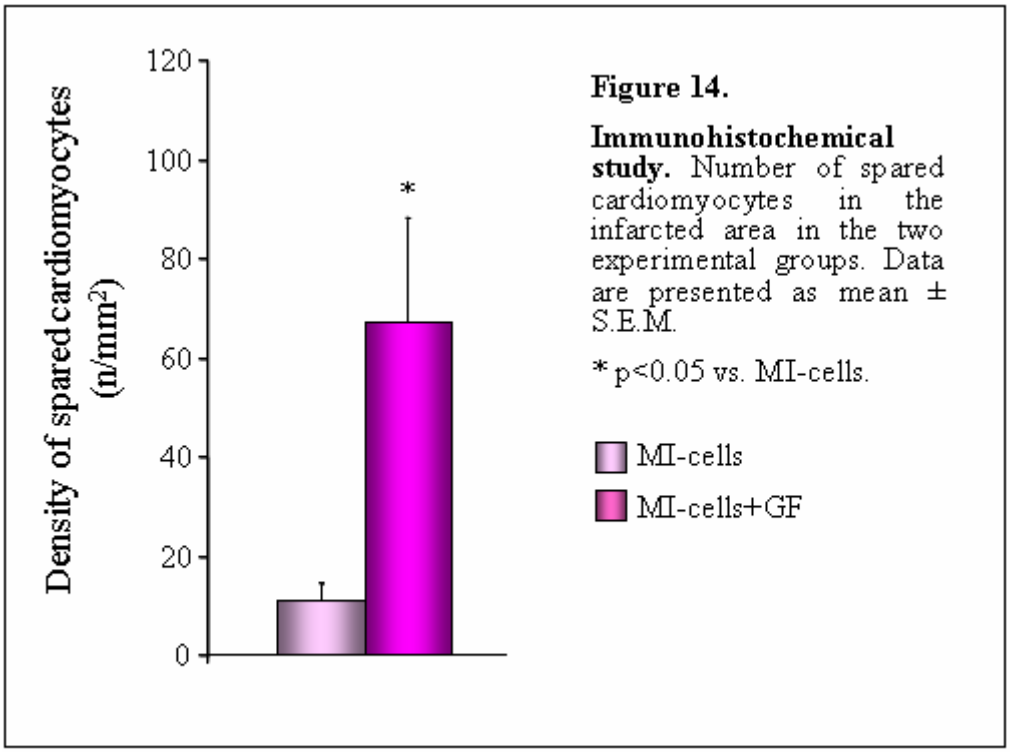

Figure 14.

Immunohistochemical study. Number of spared cardiomyocytes in the infarcted area in the two experimental groups. Data are presented as mean ± S.E.M.

* p<0.05 vs. MI-cells.

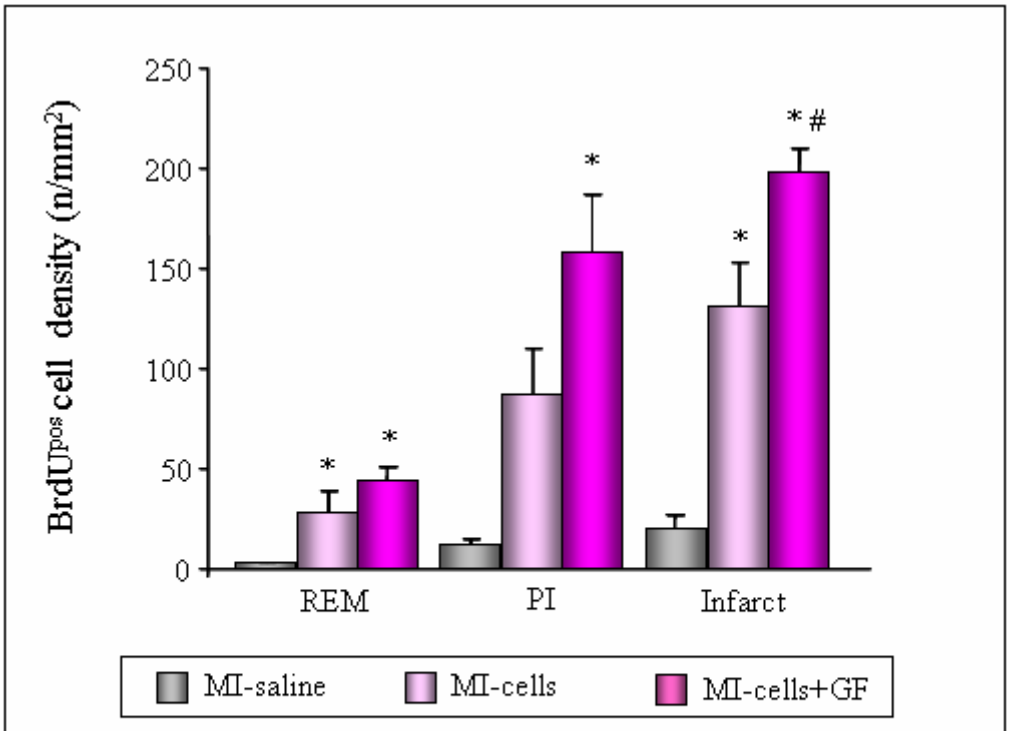

Figure 15. Immunohistochemical study. Number of BrdU^{pos} cells in the remote (REM), peri-infarcted (PI) and infarcted (infarct) areas of the experimental groups. * p<0.05 vs. MI-saline; # p<0.05 vs. MI-cells.

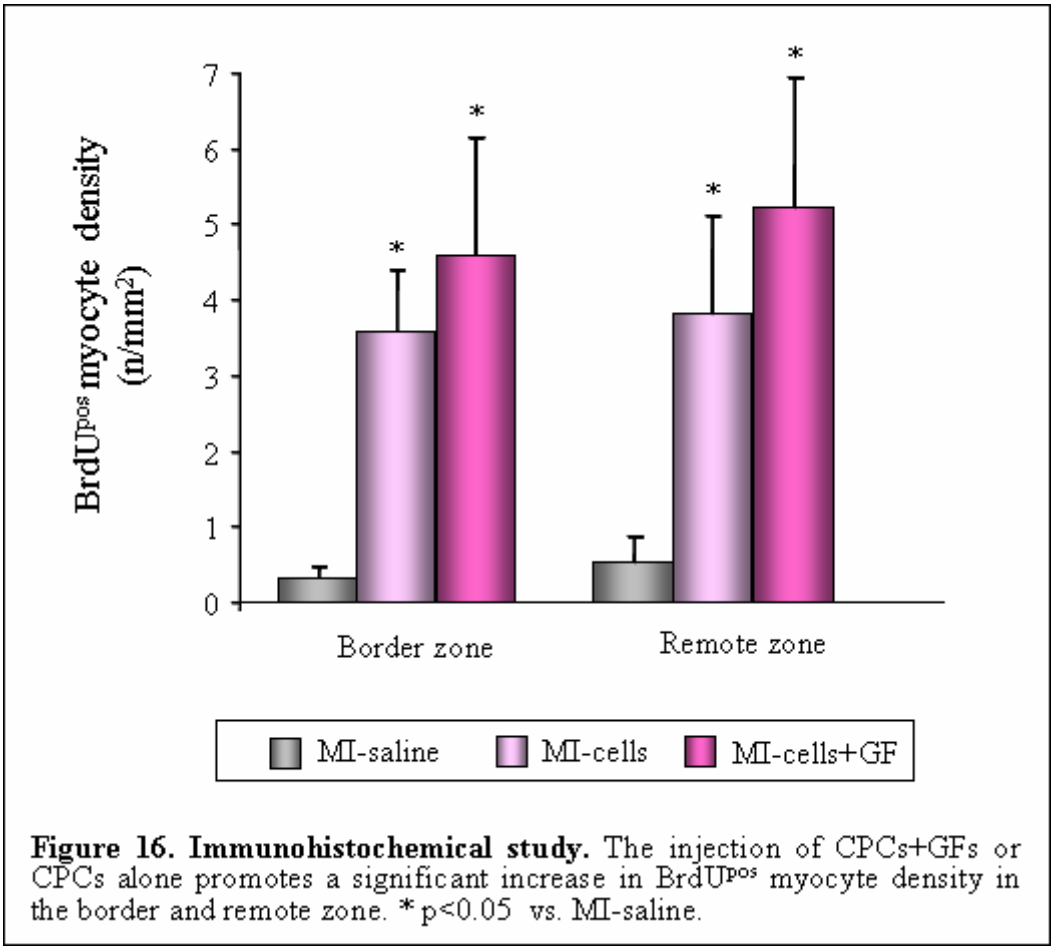

Figure 16. Immunohistochemical study. The injection of CPCs+GFs or CPCs alone promotes a significant increase in $BrdU^{pos}$ myocyte density in the border and remote zone. * $p<0.05$ vs. MI-saline.

DISCUSSION

Repairing and restoring myocardial structure and function represent ideal outcomes for the treatment of cardiomyopathies. Current therapeutic interventions rely predominantly upon pharmacologic strategies aimed at preventing the occurrence or slowing the progression of heart failure. However, the ultimate destination for many of these patients will be an operating room to receive either a cardiomyoplasty, a mechanical assist device, or a transplanted donor heart. The cost, invasiveness, shortage of suitable donor organs, and the compromised quality of life are just a few of many issues stemming from the current approaches to treating advanced heart failure. An attractive alternative vision for treating these patients could be the use of regenerative approaches that would enable the replacement and repair of the compromised tissue on a cellular level rather than exclusively prop-up damaged organ function.

Stem cell-based therapies for the treatment of myocardial damage originated from findings reported in studies on bone morrow-derived cells [61] and, more recently, on stem cells derived from the heart [24, 59]. The ultimate origin of cardiac stem cells remains speculative, but there is no dispute that such cells exert powerful recuperative effects upon the myocardium. The feasibility of adult autologous cellular therapy in acute myocardial infarction has been demonstrated in humans. However, the following questions related to the link between experimental and clinical observations remain to be solved:

- the long-term fate of transplanted stem cells in the recipient tissue;
- the ability of transplanted stem cells to find the adequate myocardial environment;
- the potency of extra-cardiac stem cells to trans-differentiate into cardiac cells;
- the complete functional integration of the regenerated myocardium with the spared tissue;
- the angiogenic background needed for transplanted cells in an ischemic tissue;
- the capability of the host tissue to allow the differentiation of engrafted cells;
-specific tracing of engrafted cells or cell populations detectable by imaging techniques.

Since research on human embryonic stem cells represents an expected future, clinical application is focusing on the use of adult stem cells to repair the damaged heart.

Recent published reports have contributed to identify the possible approaches of cellular therapy to generate new myocardium involving systemic and local mobilization

of progenitor cells. Available data on the clinical application of bone marrow progenitors or myoblasts to repair the infarcted human heart are not completely convincing. Therefore, the possibility that bone marrow derived stem cells or implantation of skeletal muscle derived myoblasts can effectively produce a complete and competent myocardium has to be tested. All these aspects including electrical-mechanical competence of the newly formed myocardium have to be considered a fundamental prerequisite for any clinical application in this field of research.

We have paid attention to these questions focusing our studies on the primitive cell populations resident in the heart and their role in cardiovascular pathologies. It is more convincing from a therapeutic prospective to establish whether pluripotent cells present in an organ can be activated in order for them to translocate to regions of damage, home within the destroyed tissue, and regenerate a healthy organ. In brief, cell turnover of organs such as the brain and the heart might be regulated by stem cell growth and differentiation. The identification of growth factors that selectively trigger stem cell translocation and proliferation may lead to the recognition of novel therapies, which could not be predicted only a few years ago. Examples of this approach exist in both the brain and the heart.

Recent data have shown that the adult heart from rat, dog, pig, and most importantly from humans, possesses a subpopulation of undifferentiated cells expressing the surface antigens c-kit, MDR-1 and SCA-1 [15-19], typically present in hematopoietic stem cells [20-23]. The finding that these cells (resident cardiac stem cells: CSCs) are able to differentiate into the three major cardiac cell types including myocytes, smooth muscle cells and endothelial cells [18, 24, 25] has dramatically challenged the generally accepted but never proven paradigm that the heart is a post-mitotic organ. The possibility to rebuild muscle, arteries and capillaries is the necessary requirement to obtain successful approaches in cardiac regeneration. Formation or implantation of a single cellular component will inevitably fail to repair the damaged organ.

Recent studies performed in rat [24] and mouse models [28] have shown that when CSCs are injected directly into the myocardium adjacent to the infarct, produced by a permanent coronary occlusion, they migrate to the infarct and reconstitute part of the dead tissue, reducing infarct size and ameliorating cardiac function. Similar results

have been obtained by intravascular delivering of CSCs, in rat models with temporary coronary occlusion followed by reperfusion [29]. Furthermore, CSCs express c-Met and insulin-like growth factor-1 (IGF-1) receptors and synthetize and secrete the corresponding ligands, hepatocyte growth factor (HGF), which mobilizes CSCs, and IGF-1, which promotes CSCs survival and proliferation [30]. The injection of HGF and IGF-1 in the infarcted hearts of dogs [30], mice [32] and rats [39] enhanced the translocation of CSCs from the surrounding myocardium to the dead tissue and their viability and growth within the damaged area. These findings suggest that cytokines capable of selectively triggering the translocation and proliferation of CSCs may be particularly suited for MI repair through the promotion of high level of organization of newly formed myocytes and vessels as well as their functional integration with the spared tissue.

Although the administration of CSCs locally or their activation by growth factors (GFs) regenerate the infarcted myocardium acutely [62, 63, 64], whether the same protocol can rescue old scarred infarcts remains an important unanswered question. This possibility would make cellular therapy more relevant to the management of human chronic heart failure.

In order for cell therapy to be widely clinically applicable, the optimal regenerative therapy has to produce new myocardium mechanically and electrically integrated with the host myocardium. Myocardial infarction (MI) is a leading cause of ventricular arrhythmias and sudden death. Cell therapy for MI using skeletal myoblasts or bone marrow-derived cells has been shown to improve cardiac mechanical function [45, 61, 65], perfusion [47], symptoms [49], and decrease infarct size [45]. While cell therapy for MI shows promise, some evidence suggests that such therapy is unable to improve electrical function and may also have a proarrhythmic effect [41]. Early clinical and experimental studies of skeletal myoblasts therapy have shown an increased incidence of ventricular arrhythmias [44, 66]. Consistent with this clinical observation, basic studies have shown that skeletal myoblasts do not electrically couple with native myocardium in-vivo [67] and when injected intramyocardially tend to cluster near injection sites [68, 69], both of which may be the basis for arrhythmias reported in clinical studies. In contrast, recent studies using bone marrow derived cells therapy [42,66,70] have not reported a significant incidence of arrhythmias. Mesenchymal stem

cells can be delivered by intravenous infusion soon after myocardial infarction and have been shown to form gap junction with host myocytes in vivo [71, 72]. Thus, mesenchymal stem cells may enhance electrical viability of the myocardium damaged by MI.

Despite the rapidity in which cellular therapy for MI has progressed from the laboratory to the clinical setting, many fundamental questions regarding the electrophysiological and arrhythmic consequences are still unresolved. Importantly, it is unknown whether cell therapy can enhance electrical viability of damaged myocardium and reduce risk of post-MI arrhythmias.

This issue was specifically addressed in the present study where we tested the hypothesis that the repair of the infarcted myocardium can significantly ameliorate both the mechanical and electrical function of the regenerated heart, in a rat model of chronic MI. The importance of studying chronic MI resides in the fact that: (i) ventricular remodeling following MI represents a major cause of late infarct-related heart failure, and (ii) lethal arrhythmias are responsible for up to half the deaths in heart failure. Two different experimental approaches were used in order to repair the infarcted myocardium: 1) in situ activation of resident progenitors by local injection of growth factors (HGF and IGF-1) and 2) local injection of CPCs with or without the addition of HGF and IGF-1. These two GFs were used to ameliorate the cell-unfriendly microenvironment that occurs after myocardial infarction. It is likely that fibrotic tissue formation leading to cardiac functional impairment precludes the effective repopulation of the injured area by exogenous cells. A strategy to provide a better regenerative environment in the damaged heart involves the use of growth factors. In particular we have chosen HGF and IGF-1 because it has been already demonstrated that HGF is a powerful chemo-attractant of CPCs [37, 38] whereas IGF-1 promotes their proliferation and survival [33, 34]. Over-expression of the IGF-1 transgene selectively in the heart promotes cardiomyocyte formation and reduces myocyte death after infarction [35,36]. Moreover, IGF-1 has been reported to increase the expression of Cx43 [73, 74] so, it may play an important role in the electrical coupling between new myocytes and spared tissue.

The proneness to arrhythmias was determined by telemetry ECG which allows the continuous recording of cardiac electrical activity in conscious freely moving

animals, avoiding the confounding effects of anesthesia. Arrhythmias were induced by submitting the rats to an acute social challenge which belongs to the real life of social animals and is known to produce an intense sympathetic stimulation potentially able to activate arrhythmogenic pathways in predisposed subjects [52].

As a whole, the results obtained in the present study indicate that the three different approaches used to induce cardiac regeneration are all able to produce a beneficial effect on structural repair of the damaged heart. This positive effect can be expected by considering that all treatments are based on mobilization and/or administration of primitive pluri-potent cells that can differentiate into the main cardiac cell lineages (myocytes, vascular smooth muscle cells, and endothelial cells), thus leading to the formation of new myocytes as well as coronary vessels, both required for reducing the unfavorable post infarction ventricular remodeling. Indeed, myocardial repair cannot be fully accomplished by cells already committed only to the myocyte lineage. Myocytes would not grow or survive in the absence of vessels. Similarly, the utilization of cells capable of creating exclusively coronary vessels cannot result in significant tissue regeneration. In addition, vessels alone do not generate force.

The first consequence of the regenerative processes was a partial (MI-GF group) or complete recovery (MI-cell and MI-cell+GF groups) of ventricular mechanical function. In accordance with previous reports [13], this effect can be ascribed to the engraftment of newly formed, functionally competent cardiac tissue which results not only in a decreased stiffness of the scarred portion of the scarred portion of the left ventricular wall but, most importantly, dynamically contributes to myocardial contractility. More pronounced functional and structural benefits were obtained when CPCs were implanted, either alone or associated with GFs. Although this could be only the consequence of the increased progenitor cell pool, implanted cells may also exert a paracrine effect activating a growth response of resident progenitor cells. Paracrine pathways due to the implanted CPCs may also explain the morpho-functional improvement observed in the remote myocardium, via the activation of other mechanisms such as inhibition of apoptosis, favorable changes in the interstitium, reduced cellular compensatory hypertrophy, etc.

As stated before, in accordance with previous data, we always found a positive remodeling of the left ventricle and beneficial hemodynamic effects, with only minor

differences among treatments. Conversely, the electrophysiological consequences of CPC mobilization/injection exhibited a clear relationship with the approach employed for cardiac repair. Specifically, the injection of progenitor cells alone (MI-cells group) was completely ineffective on arrhythmia vulnerability which remained comparable to that observed in untreated MI animals and significantly higher than in sham operated rats. Conversely, a reduction in the incidence of stress-induced ventricular arrhythmias occurred after administration of both GFs or CPCs+GFs. However, when progenitor cells were injected together with GF this protective effect was much more evident and involved all MI-cells+GF rats.

These findings can be interpreted by considering that at least two factors play a pivotal role in the recovery of the electrical competence of the damaged myocardium, i.e.: 1) the degree of electrical and mechanical coupling between the newly formed and the host tissue, potentially creating a substrate for reentry arrhythmias, and 2) the degree of cell differentiation, both in absolute terms within the newly formed tissue and relative to the spared myocytes, which may increase the heterogeneity of cellular electrophysiological properties thus favoring the occurrence of arrhythmias. Although these factors are also important for the mechanical performance of the regenerated heart, they are much more critical for the electrical performance. Our results suggest that the different electrophysiological consequences of the three regenerative treatments is mainly related to different effects on tissue heterogeneity. Indeed, all treatments led to a good integration of the newly formed tissue with the host tissue, as indicated by immunohistochemical/immunoblotting data showing, respectively, a proper spatial distribution and an increased expression of the two junctional proteins N-Cadherin and Connexin43, as compared with untreated animals. By contrast, the higher degree of cell differentiation induced by cytokines in both MI-GF and MI-cells+GF groups, presumably leading to a reduced cellular morpho-functional heterogeneity, can explain the effectiveness of these two treatments against ventricular arrhythmogenesis. The fact that this benefit was more evident when CPCs were simultaneously injected with GF might be interpreted by taking into consideration that a) the treatment provides the availability of a high number of CPCs in the damaged region which do not need to be mobilized, thus accelerating the differentiation process, and b) the implanted cells may co-operate with GFs in favoring mobilization and growth of resident CPCs by activating

paracrine pathways. We are in the process to dissect these mechanisms by evaluating (i) how GFs affect the number of engrafted cells and (ii) the different contribution of exogenous EGFP-CPCs and resident CPCs in the formation of electrically competent myocardium.

In conclusion, the contemporary injection of progenitor cells and cytokines appears to be the most suitable therapeutic approach for the recovery of mechanical as well as electrical competence of the regenerated heart in experimental chronic myocardial infarction, although more efforts have to be made to better define the underlying cellular/molecular mechanisms.

REFERENCES

1. **Nian M, Lee P, Khaper N, Liu P.** Inflammatory cytokines and postmyocardial infarction remodeling. *Circ Res* 2004; 94:1543-1553.

2. **Jessup M, Brozena S.** Heart failure. *N Engl J Med* 2003; 348:2007-2018.

3. **Losordo DW, Dimmeler S.** Therapeutic angiogenesis and vasculogenesis for ischemic disease: part II: cell-based therapies. *Circulation* 2004; 109:2692-2697.

4. **Wollert KC and Drexler H.** Clinical applications of stem cells for the heart. *Circ Res* 2005; 96:151-163.

5. **Schächinger V, Tonn T, Dimmeler S, Zeiher AM.** Bone-morrow-derived progenitor cell therapy in need of proof of concept: design of the REPAIR-AMI trial. *Nat Clin Pract Cardiovasc Med* 2006; 3 (suppl):S23-S28.

6. **Assmus B, Honold J, Schächinger V, et al.** Transcoronary transplantation of progenitor cells after myocardial infarction. *N Engl J Med* 2006;355:1222-1232.

7. **Schächinger V, Erbs S, Elsässer A, et al.** for the REPAIR-AMI Investigators. Intracoronary bone marrow-derived progenitor cells in acute myocardial infarction. *N England J Med* 2006; 355(12):1210-1221.

8. **Britten MB, Abolmaali ND, Assmus B, et al.** Infarct remodeling after intracoronary progenitor cell treatment in patients with acute myocardial infarction (TOPCARE-AMI): mechanistic insights from serial contrast-enhanced magnetic resonance imaging. *Circulation* 2003; 108:2212-2218.

9. **Meyer GP, Wollert KC, Lotz J, et al.** Intracoronary bone marrow cell transfer after myocardial infarction: eighteen months' follow-up data from the randomized, controlled BOOST (BOne marrOw transfer to enhance ST-elevation infarct regeneration) trial. *Circulation* 2006; 113:1287-1294.

10. **Welt FG, Losordo DW.** Cell therapy for acute myocardial infarction: curb your enthusiasm? *Circulation* 2006; 113:1287-1294.

11. **Boyle AJ, Schulman SP, Hare JM, et al.** Is stem cell therapy ready for patients? Stem cell therapy for cardiac repair. Ready for the next step. *Circulation* 2006. 114:339-352.

12. **Anversa P, Kajstura J, Leri A, Bolli R.** Life and death of cardiac stem cells: a paradigm shift in cardiac biology. *Circulation* 2006; 113:1451-1463.

13. **Anversa P, Leri A, Kajstura J.** Cardiac regeneration. *J Am Coll Cardiol.* 2006; 47:1769-1776.

14. **Leri A, Kajstura J, Anversa P.** Cardiac stem cells and mechanisms of myocardial regeneration. *Physiol Rev* 2005; 85:1373-1416.

15. **Chimenti S, Barlucchi L, Limana F, et al.** Local mobilization of resident cardiac primitive cells by growth factors repairs the infarcted heart. *Circulation* 2002;106:II-14.

16. **Cesselli D, Kajstura J, Jakoniuko I, et al.** Cardiac stem cells (CSC) are endowed in niches of the adult mouse heart and possess the ability to divide and differentiate in the various cardiac lineages. *Circulation* 2002; 106:II-286.

17. **Anversa P, Nadal-Ginard B.** Myocyte renewal and ventricular remodelling. *Nature* 2002; 415:240-243.

18. **Quaini F, Urbanek K, Beltrami AP, et al.** Chimerism of the transplanted heart. *N Engl J Med* 2002; 346:5-15.

19. **Urbanek K, Quaini F, Bussani R, et al.** Cardiac stem cells (CSC) growth and death differ in acute and chronic ischemic heart failure in humans. *Circulation* 2002; 106:II-383.

20. **Fuchs E, Segre JA.** Stem cells: a new lease on life. *Cell* 2000; 100:143-155.

21. **Bunting KD.** ABC transporters as phenotypic markers and functional regulators of stem cells. *Stem Cells* 2002; 20:11-20.

22**. Blau HM, Brazelton TR, Weimann JM.** The evolving concept of a stem cell: entity or function? *Cell* 2001; 105:829-841.

23. **Sellers SE, Tisdale JF, Agricola BA, et al.** The effect of multidrug-resistence 1 gene versus neo transduction on ex vivo and in vivo expansion of rhesus macaque hematopoietic repopulating cells. *Blood* 2001; 97:1888-1891.

24. **Beltrami AP, Barlucchi L, Torella D, et al.** Adult cardiac stem cells are multipotent and support myocardial regeneration. *Cell* 2003; 114:763-776.

25. **Urbanek K, Quaini F, Tasca G, et al.** Intense myocyte formation from cardiac stem cells in human cardiac hypertrophy. *Proc Natl Acad Sci USA* 2003; 100:10440-10445.

26. **Pomerantz J, Blau HM.** Nuclear reprogramming: a key to stem cell function in regenerative medicine. *Nat Cell Biol* 2004; 6:810-816.

27. **Leri A, Kajstura J, Anversa P.** Identity deception: not a crime for a stem cell. *Physiolgy* 2005; 20:162-168.

28. **Messina E, De Angelis L, Frati G, et al.** Isolation and expansion of adult cardaic stem cells from human and murine heart. *Circ Res* 2004; 95:911-921.

29. **Dawn B, Stein AB, Urbanek K, et al**. Cardiac stem cells delivered intravascularly traverse the vessel barrier, regenerate infarcted myocardium, and improve cardiac function. *Proc Natl Acad Sci USA* 2005; 102:3766-3771.

30. **Linke A, Muller P, Nurzynska D, et al.** Stem cells in the dog heart are self-renewing, clonogenic, and multipotent and regenerate infarcted myocardium, improving cardiac function. *Proc Natl Acad Sci USA* 2005; 102:8966-8971.

31. **Limana F, Germani A, Zacheo A, et al.** Exogenous high-mobility group box 1 protein induces myocardial regeneration after infarction via enhanced cardiac c-kit+ cell proliferation and differentiation. *Circ Res* 2005; 97:e73-e83.

32. **Urbanek K, Rota M, Cascapera S, et al.** Cardiac stem cells possess growth factor-receptor systems that after activation regenerate the infarcted myocardium, improving ventricular function and long-term survival. *Circ Res* 2005; 97:663-673.

33. **Arsenijevic Y, Weiss S, Schneider B, Aebischer P.** Insulin-like growth factor-1 is necessary for neural stem cell proliferation and demonstrates distinct actions of epidermal growth factor and fibroblast growth factor-2. *J Neurosci* 2001; 21:7194-7202.

34. **Li Q, Li B, Wang X, et al.** Overexpression of insulin-like growth factor-1 in mice protects from myocyte death after infarction, attenuating ventricular dilation, wall stress, and cardiac hypertrophy. *J Clin Invest* 1997; 100:1991-1999.

35. **Torella D, Rota M, Nurzynska D, et al.** Cardiac stem cell and myocyte aging, heart failure, and insulin-like growth factor-1 overexpression. *Circ Res* 2004; 94:514-524.

36. **Capogrossi MC.** Cardiac stem cells fail with aging: a new mechanism for the age-dependent decline in cardiac function. *Circ Res* 2004; 94:411-413.

37. **Powell EM, Mars WM, Levitt P.** Hepatocyte growth factor/scatter factor is a motogen for interneurons migrating from the ventral to dorsal telencephalon. *Neuron* 2001; 30:79-89.

38. **Hamasuna R, Kataoka H, Moriyama T, et al.** Regulation of matrix metalloproteinase-2 (MMP-2) by hepatocyte growth factor/scatter factor (HGF/SF) in human glioma cells: HGF/SF enhances MMP-2 expression and activation, accompanying up-regulation of membrane type 1 MMP. *Int J Cancer* 1999; 82:274-281.

39. **Rota M, Padin-Iruegas ME, Misao Y, et al.** Local activation or implantation of cardiac progenitor cells rescues scarred infarcted myocardium improving cardiac function. *Circ Res* 2008; 103:107-116.

40. **Anversa P, Sussman MA, Bolli R.** Molecular genetic advances in cardiovascular medicine: focus on the myocyte. *Circulation* 2004; 109:2832-2838.

41. **Makkar RR, Lill M, Chen PS.** Stem cell therapy for myocardial repair: is it arrhythmogenic? *J Am Coll Cardiol* 2003; 42:2070-2072.

42. **Smits PC, van Geuns RJ, Poldermans D, et al.** Catheter-based intramyocardial injection of auotologous skeletal myoblasts as a primary treatment of ischemic heart failure: clinical experience with six-month follow-up. *J Am Coll Cardiol* 2003; 42:2063-2069.

43. **Menasché P, Hagège AA, Scorsin M, et al.** Myoblast transplantation for heart failure. *Lancet* 2001; 357:279-280.

44. **Menasché P, Hagège AA, Vilquin JT, et al.** Autologous skeletal myoblast transplantation for severe postinfarction left ventricular dysfunction. *J Am Coll Cardiol* 2003; 41:1078-1083.

45. **Strauer BE, Brehm M, Zeus T, et al.** Repair of infarcted myocardium by autologous intracoronary mononuclear bone marrow cell transplantation in humans. *Circulation* 2002; 106:1913-1918.

46. **Assmus B, Schachinger V, Teupe C, et al.** Transplantation of progenitor cells and regeneration enhancement in acute myocardial infarction (TOPCARE-AMI). *Circulation* 2002; 106:3009-3017.

47. **Stamm C, Westphal B, Kleine HD, et al.** Autologous bone-marrow stem-cell transplantation for myocardial regeneration. *Lancet* 2003; 361:45-46.

48. **Perin EC, Dohmann HF, Borojevic R, et al.** Transendocardial, autologous bone marrow cell transplantation for severe, chronic ischemic heart failure. *Circulation* 2003; 107:2294-2302.

49. **Tse HF, Kwong YL, Chan JK, et al.** Angiogenesis in ischaemic myocardium by intramyocardial autologous bone marrow mononuclear cell implantation. *Lancet* 2003; 361:47-49.

50. **Martinez M, Calvo Torrent A, Pico Alfonso MA.** Social defeat and subordination as models of social stress in laboratory rodents: a review. *Aggress Behav* 1998; 24:241–256.

51. **Sgoifo A, Stilli D, Medici D, et al.** (1996*b*). Electrode positioning for reliable telemetry ECG recordings during social stress in unrestrained rats. *Physiol Behav* 1996; 60:1397–1401.

52. **Sgoifo A, De Boer SF, Haller J, Koolhaas JM.** Individual differences in plasma catecholamine and corticosterone stress responses of wild-type rats: relationship with aggression. *Physiol Behav* 1996; 60:1403–1407.

53. **M. Okabe, M. Ikawa, K. Kominami, et al.** 'Green mice' as a source of ubiquitous green cells. *FEBS Lett* 1997; 407:313–319.

54. **Leri A, Liu Y, Wang X, et al.** Overexpression of insulin-like growth factor-1 attenuates the myocyte renin-angiotensin system in transgenic mice. *Circ Res* 1999; 84:752-762.

55. **Dodge HT, Baxley WA.** Left ventricular volume and mass and their significance in heart desease. *Am J Cardiol.* 1969; 23:528-537.

56. **Bearzi C, Rota M, Hosoda T, et al.** Human cardiac stem cells. *Proc Natl Acad Sci USA* 2007;104:14068-14073.

57. **Anversa P, Olivetti G.** Cellular basis of physiological and pathological myocardial growth. In: Page E, Fozzard H, Solaro RJ, eds. *Handbook of Physiology*. *The Cardiovascular system: The Heart.* New York, NY: Oxford University Press; 2002:75-144.

58. **Stilli D, Bocchi L, Berni R, et al.** Correlation of α-skeletal actin expression, ventricular fibrosis and heart function with the degree of pressure overload cardiac hypertrophy in rats. *Exp Physiol* 2006**;** 91:571-580.

59. **Orlic D, Kajstura J, Chimenti S, et al.** Mobilized bone marrow cells repair the infarcted heart, improving function and survival. *Proc Natl Acad Sci USA* 2001; 98:10344-10349.

60. **Berni R, Cacciani F, Zaniboni M, et al**. Effects of the α2-Adrenergic/DA2-dopaminergic agonist CHF-1024 in preventing ventricular arrhythmogenesis and myocyte electrical remodelling, in a rat model of pressure-overload cardiac hypertrophy. *J Cardiovasc Pharmacol* 2006; 47:295-302.

61. **Orlic D, Kajstura J, Chimenti S, et al.** Bone marrow cells regenerate infarcted myocardium. *Nature* 2001; 410:701-705.

62. **Rota M, Boni A, Urbanek K, et al.** Nuclear targeting of Akt enhances ventricular function and myocytes contractility. *Circ Res* 2005; 97:1332-1341.

63. **Lanza R, Moore MA, Wakayama T, et al.** Regeneration of the infarcted heart with stem cells derived by nuclear transplantation. *Circ Res* 2004; 94:820-827.

64. **Rota M, LeCapitaine N, Hosoda T, et al.** Diabetes promotes cardiac stem cell aging and heart failure, which are prevented by deletion of the p66shc gene. *Circ Res* 2006; 99:42-52.

65. **Yau TM, Tomita S, Weisel RD, et al.** Beneficial effect of autologous cell transplantation on infarcted heart function:comparison between bone marrow stromal cells and heart cells. *Ann Thorac Surg* 2003; 75:169-76.

66. **Fernandes S, Amirault JC, Lande G, et al.** Autologous myoblasts transplantation after myocardial infarction increases the inducibility of ventricular arrhythmias. *Cardiovasc Res* 2006; 69:348-358.

67. **Reinecke H, MacDonald GH, Hauschka SD, et al.** Electromechanical coupling between skeletal and cardiac muscle. Implication for infarct repair. *J Cell Biol* 2000; 149:731-40.

68. **Fouts KH, Fernandes B, Mal N, et al.** Electro physiological consequences of skeletal myoblast transplantation in normal and infarcted canine myocardium. *Heart Rhythm* 2006; 3:452-61.

69. **Thompson RB, Emani SM, Davis BH, et al.** Comparison of intracardiac cell transplantation: autologous skeletal myoblasts versus bone marrow cells. *Circulation* 2003; 108 (suppl 1): II264-71.

70. **Wollert KC, Meyer GP, Lotz J, et al.** Intracoronary autologous bone-marrow cell transfer after myocardial infarction: the BOOST randomised controlled clinical trial. *Lancet* 2004; 364:141-8.

71. **Valiunas V, Doronin S, Valiuniene L, et al.** Human mesenchymal stem cells make cardiac connexins and form functional gap junctions. *J Physiol* 2004; 555:617-26.

72. **Patapova I, Plotnikov A, Lu Z, et al.** Human mesenchymal stem cells as a gene delivery system to create cardiac pacemakers. *Circ Res* 2004; 94:952-9.

73. **Aberg ND, Blomstrand F, Aberg MA, et al.** Insuline-like growth factor-I increases astrocyte intercellular gap junctional communication and connexin43 expression in vitro. *J Neurosci Res* 2003: 74:12-22.

74. **Doble BW, Kardami E.** Basic fibroblast growth factor stimulates connexion-43 expression and intercellular communication of cardiac fibroblasts. *Moll Cell Biochem* 1995: 143:81-87.